

MOLECULAR DYNAMICS IN FEMTOCHEMISTRY AND FEMTOBIOLOGY

JOSHUA JORTNER AND M. BIXON
*School of Chemistry, Tel Aviv University,
Ramat Aviv, 69978 Tel Aviv, Israel*

This paper addresses the conceptual framework of femtosecond chemistry and biology which rests on a unified theory and simulation of intramolecular, cluster, condensed phase and biophysical dynamics with the temporal resolution of atomic motion.

1. On dynamics

We shall be concerned with femtosecond dynamics in isolated molecules, clusters, condensed phase and biosystems, which pertains to the elucidation of the phenomena of energy acquisition, storage and disposal as explored from the microscopic point of view. The broad area of nonradiative dynamics, from small molecules to biomolecules, played a central role in the development of modern chemistry during this century. This can be artistically described as ascending the 'magic mountain' of molecular, cluster condensed phase and biophysical dynamics by several paths (Fig. 1), all of which go heavenwards towards a unified and complete description of structure-electronic level structure-energetic-spectroscopic-dynamic relations and correlations.

The genesis of intramolecular nonradiative dynamics dates back to the origins of quantum mechanics. In 1928 Bonhoeffer and Farkas¹ observed that predissociation in the electronically excited ammonia molecule, which involves the decay of a metastable state to a dissociative continuum, i.e., $\text{NH}_3 \xrightarrow{h\nu} \text{NH}_3^* \xrightarrow{1/\tau} \text{NH}_2 + \text{H}$, is manifested by spectral line broadening (linewidth Γ), establishing the first spectroscopic-dynamic relation. This observation provided experimental verification of the Heisenberg energy-time uncertainty relation $\Gamma\tau \sim h$, with the decay lifetime τ being quantified in terms of the golden rule² $\tau^{-1} = (4\pi^2/h)|H|^2(dn/dE)$, where H is the matrix element of the perturbation causing the transition, and dn/dE is the energy density of states. Important developments in the realm of intermolecular dynamics were pioneered by Polanyi and Wigner in the 1930s,³ for kinetics in the gas phase, in molecular beams and in solution.⁴ A distinct field of dynamics in the condensed phase was pioneered by Kubo⁵ and by Marcus⁶ in the 1950s. Kubo and Toyozawa⁵ considered electron-hole recombination in semiconductors which constitutes a somewhat esoteric example of electron transfer and resulted in a free-energy (ΔG) relation for the rate (k). The Gaussian free-energy relation $k \propto \exp[-(\Delta G + \lambda)^2/4\lambda k_B T]$

(where λ is the medium reorganization energy) constitutes a cornerstone of the Marcus theory of electron transfer.⁶ Conceptually and physically isomorphous classes of dynamics pertain to the Marcus theory of electron transfer⁶ and to the Förster theory of electronic energy transfer in solutions, solids and glasses.⁷ The extension of dynamics to protein media emerged with the development of biophysical dynamics in the 1960s, with the experimental studies of electron transfer in photosynthesis.⁸ Cluster dynamics, which constitutes the borderline between molecular and condensed phase phenomena, emerged in the 1970s.^{9,10} During the last decade the advent of femtosecond ultrafast dynamics^{11,12} allowed for the exploration of radiationless processes in chemical and biophysical systems, with the temporal resolution of atomic motion, exerting a major impact on all the paths of dynamics portrayed in Fig. 1.

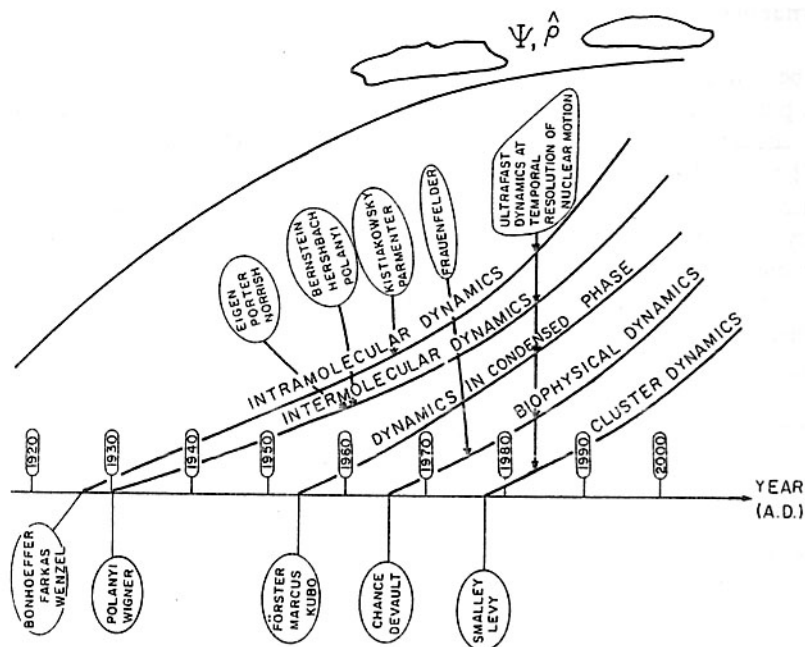


Fig. 1. An artist's view of the 'magic mountain' of the evolution of molecular, cluster, condensed phase and biophysical dynamics during this century. The names of some of the pioneers who initiated each scientific area are marked on the path.

Femtosecond dynamics opened up new horizons in the exploration of ultrafast radiationless processes. These involve isolated molecules, where ultrafast 'nonreactive' intramolecular internal conversion can occur on the time scale of

vibrational motion, while 'reactive' dissociation^{13,14} and Coulomb explosion^{15,16} manifest the sliding down on the repulsive nuclear surface. In some cluster and condensed phase systems ultrafast energy dissipation processes, manifesting collective large nuclear configurational changes, bear analogy to molecular 'reactive' dynamics, but can concurrently maintain vibrational phase coherence induced by nuclear impact. For ultrafast dynamics in clusters, in the condensed phase and in the protein medium, separation of time scales for nuclear dynamics may prevail.¹⁵ Interstate and energy relaxation are understood, while the interplay between relaxation and dephasing is of considerable interest. The ubiquity of vibrational and electronic coherence effects, ranging from small to huge systems,^{11,12,17-20} raises the conceptual question of the distinction between the experimental conditions of the preparation and interrogation, and the intrinsic aspects of relaxation and dephasing dynamics. These are some of the central aspects of the novel and fascinating area of femtochemistry, whose conceptual framework rests on the theory and simulation of intramolecular, cluster, condensed phase and biophysical dynamics.

Theory played a central role in establishing the conceptual framework of dynamics in chemistry and biology. From the historical perspective theoretical chemistry, until the 1960s, focused on the nature of the chemical bond. This was beautifully reflected in the address of Charles Coulson at the Boulder Conference on Molecular Structure Calculations in 1959,²¹ where the goals of theoretical chemistry at that time were defined:

"We may hope that eventually all problems (of molecular structure) in the range of 1-20 electrons will be solved accurately by computational techniques... But surely there is much more in chemistry than covered by this range."²¹

Contemporary quantum chemistry has undergone major developments and currently predictions of static molecular structure, molecular properties and intramolecular interactions at the level of chemical accuracy are becoming available. But there is much more in chemistry! The theory of intramolecular, cluster, condensed phase, and biophysical dynamics developed during the last three decades, has been decisive in providing models, insight, information and prediction. Furthermore, without dynamics one cannot understand the function in chemistry and biology. The theory of chemical and biophysical dynamics on the microscopic level, relating structure, function and dynamics, had an audible impact on the development of modern chemistry.

2. Intramolecular dynamics

We start from the genesis of modern intramolecular dynamics. In 1965 the research area of intramolecular dynamics in large isolated molecules originated from the

experiments of Kistiakowski and Parmenter,²² which demonstrated the occurrence of intersystem crossing (i.e., singlet (S) - triplet (T) radiationless transition) in the 'isolated' collision-free benzene molecule. By studying the effect of cyclohexane pressure on the fluorescence quantum yield (Y) of benzene vapor it was established that $Y = 0.34$ at zero pressure. The iconoclastic implications of their results were fully realized by Kistiakowski and Parmenter, who stated that:

"a strictly intramolecular, i.e., free of collisional perturbations, nonradiative transition between pure singlet and triplet stationary states is difficult to reconcile with concepts of quantum mechanics."²²

What is so surprising about these results? Let us allude to the Pauling-Wilson discussion of the resonance phenomenon.²³ For the resonance coupling V_{ST} between a pair of singlet $|S\rangle$ triplet $|T\rangle$ states with the initial state $\Psi(0) = |S\rangle$, the time evolution of the system $\Psi(t) = A(t)|S\rangle + B(t)|T\rangle$ yields the time-dependent probabilities $\rho_{SS}(t)$ of the singlet and $\rho_{TT}(t)$ of the triplet state, i.e.,

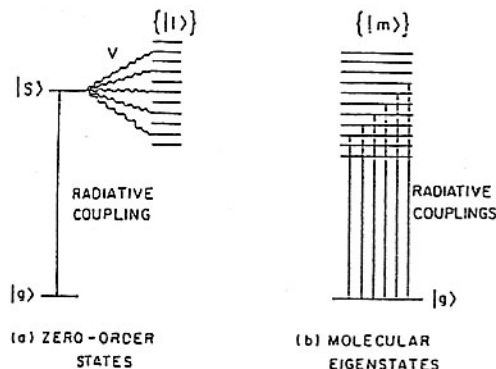
$$\begin{aligned}\rho_{SS}(t) &= \cos^2(V_{ST}t/\hbar) \\ \rho_{TT}(t) &= \sin^2(V_{ST}t/\hbar)\end{aligned}\quad (2.1)$$

In the bound level structure for the S-T coupling, as inferred from the celebrated Jablonski diagram,²⁴ an oscillatory time dependence of the population of S is thus expected and no relaxation is exhibited. Such an oscillatory time evolution, referred to as quantum beats, was predicted in 1968 by Jortner and Berry²⁵ and by Bixon, Dothan and Jortner²⁶ (section 3.4), and was experimentally observed in 1982 by Kommandeur et al²⁷ and by Zewail et al²⁸ for some cases of sparse coupled S_1 - T_1 level structure. But Kistiakowski and Parmenter²² observed a genuine decay and not temporal oscillations in the bound S_1 - T_1 level structure of the 'isolated' benzene. The intramolecular nature of radiationless transitions was established by the Bixon-Jortner model,²⁹⁻³⁴ (Fig. 2), which rests on near-resonance coupling between (zero-order) states consisting of a doorway state accessible for excitation and a background vibronic manifold, on the introduction of the concept of molecular eigenstates, on the dynamics of wavepackets of molecular eigenstates, on finite-time evolution and on practical irreversibility in a bound level structure. This general conceptual framework is applicable both for interstate coupling, which involves two electronic configurations coupled by nuclear momenta (the breakdown of the Born-Oppenheimer separability), or/and spin-orbit interaction (i.e., internal conversion and intersystem crossing), as well as for intrastate coupling, which involves a single electronic configuration with vibrational-rotational states coupled by anharmonic or coriolis interactions (i.e., intramolecular vibrational energy redistribution).

The ladder diagrams for intramolecular coupling and dynamics (Fig. 2) focus on zero-order molecular levels, i.e., the ground state $|g\rangle$, the doorway state $|s\rangle = \hat{\mu}|g\rangle$

(where $\hat{\mu}$ is the dipole operator) and the quasicontinuum manifold $\{|\ell\rangle\}$ with the density of states ρ_ℓ , with the intramolecular couplings $V_{s\ell} = \langle s|\hat{H}| \ell\rangle$, which are used to construct the molecular eigenstates

Fig. 2. A molecular energy-levels model used to describe coupling and nonreactive relaxation in a bound-level structure in excited states of large molecules. This model was introduced by Bixon and Jortner (1968) to describe interstate coupling and relaxation, and is also adequate to describe intrastate coupling and intramolecular vibrational energy redistribution.



$$|m\rangle = a_s^{(m)}|s\rangle + \sum_{\ell} b_{\ell}^{(m)}|\ell\rangle, \quad (2.2)$$

which diagonalize the system's Hamiltonian with energies E_m . The initial excitation of the doorway state, i.e., $\Psi(0) = |s\rangle$, results in the time evolution of the system

$$\Psi(t) = \sum_m a_s^{(m)}|m\rangle \exp(-iE_m t / \hbar), \quad (2.3)$$

manifesting wavepacket dynamics, with the doorway state population probability

$$P^{(D)}(t) = \left| \sum_m a_s^{(m)} \exp(-iE_m t / \hbar) \right|^2, \quad (2.4)$$

which constitutes a Fourier sum of the molecular eigenstates accessibility amplitudes $|a_s^{(m)}|^2$ (i.e., the spectrum). For strong coupling, i.e., $V_{s\ell}\rho_\ell \gg 1$, the statistical limit is realized on the time scale $t < \hbar\rho_\ell$. The spectral lineshape is Lorentzian with the

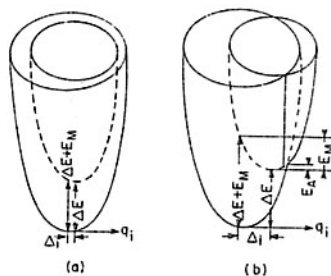
width $\Gamma = 2\pi V_{sf}^2 \rho_f$, the temporal decay of the doorway state is exponential, i.e., $P^{(D)}(t) = \exp[-(1/\tau_{\text{rad}} + 1/\tau)t]$, with the nonradiative lifetime $\tau = \hbar/\Gamma$ and τ_{rad} is the radiative lifetime.²⁹⁻³⁴ The theory²⁹⁻³³ provides the dynamic and spectroscopic implications, i.e., intrinsic spectral linebroadening and relaxation in a bound level structure of an isolated large molecule. This theory was first met with formidable resistance. Herzberg³⁵ argued that spectral linebroadening can arise only from a 'reactive' nonradiative process, e.g., predissociation or autoionization, and that it is difficult to envision relaxation in a bound level structure. In the 1969 Reunion de la Société de Chimie Physique on Nonradiative Transitions in Molecules,³⁶ the physical picture for the intramolecular bound quasicontinuum was accepted.

"Dr. Herzberg was also particularly struck by the discussion which clearly showed that internal conversion follows similar theoretical relations as do actual decomposition processes such as predissociation and preionization."³⁵

The second opposition to the theory was raised by Teller at the Farkas Memorial Symposium in 1969.³⁷ Teller invoked the notion of curve crossing, suggesting that internal conversion in a large molecule will occur near a conical intersection of two potential surfaces.³⁷ The ditochomy between the Teller picture of curve crossing in large molecules and the Bixon-Jortner model was resolved by Englman and Jortner³⁸ who have advanced two coupling limits (Fig. 3). The strong coupling limit, where the two potential energy surfaces cross in the vicinity of the minimum of the higher surface, can be realized for some intramolecular isomerization processes and for some cases of intermolecular coupling to exterior medium modes. In the weak coupling limit the displacement of the minima of the two surfaces is small so that the dynamics occurs in the region where no surface crossing prevails. This state of affairs bears analogy to nuclear tunneling. Interstate and intrastate intramolecular dynamics in a large molecule corresponds to the weak coupling situation where the nonradiative transition probability $W = 1/\tau$ from the electronic origin is given for (two) harmonic equal frequency potential surfaces by³⁸⁻⁴⁰

$$W = \left(\frac{V_{sf}^2}{\hbar^2} \right) \exp(-G) \int_{-\infty}^{\infty} dt \exp [(i\Delta E t / \hbar) + G_+(t)] \quad (2.5)$$

Fig. 3. The Englman-Jortner (1970) representation of the weak coupling limit (a) and the strong coupling limit (b) of two adiabatic potential surfaces. Interstate and intrastate coupling in large isolated molecules correspond to the weak coupling situation.



where $G_+(t) = \sum_j (\Delta_j^2 / 2) \exp(i\omega_j t)$ and the electronic-vibrational coupling strength $G = G_+(0)$. $\{\omega_j\}$ are the 'vibrational' frequencies, $\{\Delta_j\}$ are the reduced displacements of the potential surfaces minima and ΔE is the energy gap (Fig. 3). In the relevant weak coupling limit, Eq. (2.5) results in the exponential energy gap law³⁸⁻⁴⁰

$$W \propto \exp(-\gamma \Delta E / \hbar \omega_M) \quad , \quad (2.6)$$

where ω_M is an average frequency and γ a numerical constant. A more elaborate analysis of the energy gap law⁴¹ reveals that the ΔE dependence of W is superexponential but considerably slower than the Gaussian ΔE dependence, which is the case for the strong coupling limit. The universality of the exponential energy gap law, Eq. (2.6), for radiationless electronic-vibrational relaxation was established for a variety of intramolecular, as well as condensed phase, radiationless processes, which involve intersystem crossing and internal conversion in isolated large molecules and in large molecules in solution, relaxation of lanthanide complexes in crystals, electronic energy transfer, electron transfer in isolated supermolecules and electron transfer in solvated ion pairs, complexes and supermolecules.^{41,42}

Going back to general theory of intramolecular dynamics in a bound level structure, developed by Bixon, Nitzan, Mukamel and Jortner,^{26,42-50} the central ingredients are:

- (1) The characterization of the level structure. This requires the characterization of the appropriate zero-order states and their (small) couplings.
- (2) The accessibility of the zero-order states, leading to the specification of the doorway state(s) of the system.
- (3) The decay channels of the zero-order states, specifying their decay to genuine (radiative decay, predissociation, autoionization) continuum channels, which are characterized by appropriate decay widths.
- (4) The excitation initial conditions, which are governed by the (optical) excitation modes.

Ingredients (1) and (3) allow for the construction of the (complex) molecular eigenstates, i.e., the independently decaying molecular levels $\{|m\rangle\}$, which are obtained from the diagonalization of the effective Hamiltonian^{26,42,45,49,50-52}

$$H_{\text{eff}} = H_M - (i/2)\Gamma \quad , \quad (2.7)$$

where H_M is the molecular Hamiltonian and Γ is the decay matrix (Fig. 4). The $\{|m\rangle\}$ states are characterized by the complex energies

$$\epsilon_m = E_m - (i/2)\gamma_m, \quad (2.8)$$

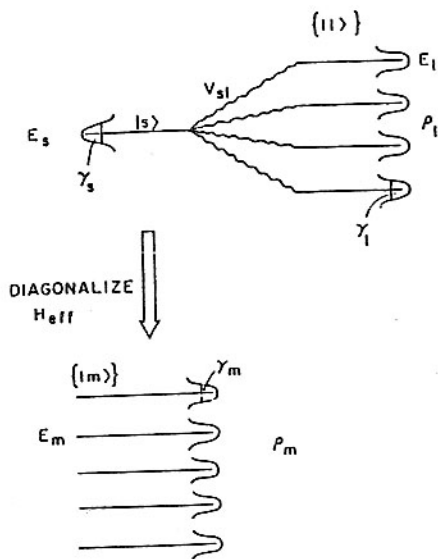
where $\{E_m\}$ are the energy levels, while $\{\gamma_m\}$ represent the decay widths. Relevant time-resolved observables for a broad-band excitation, which are based on ingredients (1) and (2), involve the population probability of the doorway state

$$P^{(D)}(t) = \left| \sum_m |A_m|^2 \exp\left(-\frac{iE_m t}{\hbar} - \frac{\gamma_m t}{2\hbar}\right) \right|^2, \quad (2.9)$$

where $A_m = \langle g | \hat{\mu} | m \rangle$ are the excitation amplitudes of the $\{|m\rangle\}$ manifold, and the energy-resolved (radiative) decay probability to a vibrational level $|gv\rangle$ of the ground electronic state

$$P^{(v)}(t) = \left| \sum_m A_m B_m^v \exp\left(\frac{-iE_m t}{\hbar} - \frac{\gamma_m t}{2\hbar}\right) \right|^2, \quad (2.10)$$

Fig. 4. The application of the effective Hamiltonian formalism for interstate and intrastate intramolecular coupling and dynamics. The zero-order states $|s\rangle$ and $\{|\ell\rangle\}$ are characterized by the energies E_s and $\{E_\ell\}$, respectively, and by the decay widths γ_s and $\{\gamma_\ell\}$. $V_{s\ell}$ represents the intramolecular (interstate or intrastate) coupling between the doorway state $|s\rangle$ and the $\{|\ell\rangle\}$ manifold, which is characterized by the density of states ρ_ℓ . Diagonalization of the effective Hamiltonian results in a set of independently decaying levels $\{|m\rangle\}$, i.e., generalized molecular eigenstates, characterized by energies $\{E_m\}$, decay widths $\{\gamma_m\}$, and density of states ρ_m .



where $B_m^v = \langle m | \hat{\mu} | gv \rangle$ are the transition amplitudes. These probabilities constitute Fourier sums damped by real decay exponents, Eqs. (2.9) and (2.10), and may involve either a superposition of exponentials (for a sparse or intermediate level

structure) or an exponential decay of a giant resonance (in the statistical limit), while Eq. (2.10) may also result in quantum beats (in the intermediate level structure). The character and dynamical manifestations of the sparse, intermediate and statistical level structure (Fig. 5) can be inferred in a transparent way from the lineshapes $L(E) = -\text{Im}G(E)$, where the Green's function is $G(E) = (E - H_{\text{eff}})^{-1}$. The classification of the level structures (Fig. 5) is specified by the coarse grained interstate or intrastate coupling V , by the density of states of the proper symmetry ρ , and by the decay widths γ .^{42,49-52} The limit of isolated states, with $V\rho < 1$, constitutes the spectroscopist's paradise, when distinct 'pure' rotational-vibrational levels can be observed. For the strongly coupled situation, with $V\rho > 1$, the sparse ($\gamma\rho < 1$), the intermediate ($\gamma\rho \sim 1$) and the statistical ($\gamma\rho \gg 1$) level structures (Fig. 5), can be realized.

3. Intramolecular relaxation, mode selectivity, quantum beats and vibronic and electronic chemistry

Some of the aspects of the theory relevant to ultrafast dynamics in isolated molecules will now be addressed.

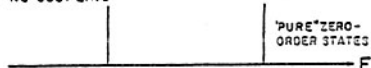
CLASSIFICATION OF LEVEL STRUCTURE

V - INTERSTATE OR INTRASTATE
COUPLING
 ρ - DENSITY OF STATES
 γ - DECAY WIDTHS

1. "ISOLATED" STATES

$V\rho < 1$ NO COUPLING

'PURE' ZERO-
ORDER STATES



2. SPARSE COUPLED LEVEL STRUCTURE

$V\rho > 1$
 $\gamma\rho \ll 1$

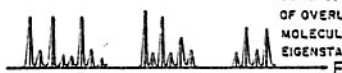
MIXED
WELL SEPARATED
MOLECULAR
EIGENSTATES



3. INTERMEDIATE LEVEL STRUCTURE-DENSE

$V\rho > 1$
 $\gamma\rho \sim 1$

BUNCHES
OF OVERLAPPING
MOLECULAR
EIGENSTATES



4. STATISTICAL LIMIT

$V\rho > 1$
 $\gamma\rho \gg 1$

STRUCTURE
SMEARED
LORENTZIAN
LINESHAPE

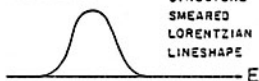
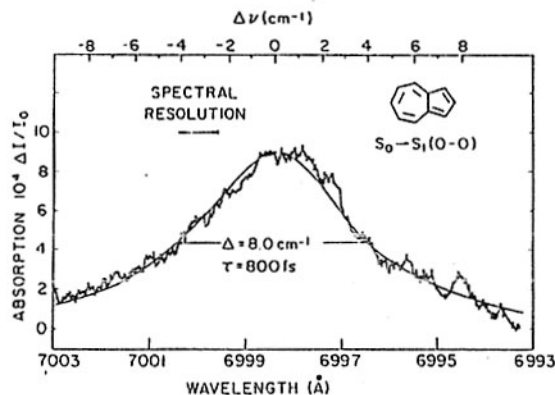


Fig. 5. Classification of the intramolecular level structure. The relevant energetic and dynamic parameters are: the (interstate or intrastate) coupling V , the density of the independently decaying levels ρ and their decay widths γ . The spectra exhibit the energy dependent lineshapes $L(E)$ vs E .

3.1 Ultrafast intramolecular relaxation in the statistical limit. The statistical limit corresponds to the extreme situation of overlapping resonances, where the whole structure in the spectrum is washed out (Fig. 5). The absorption lineshape is Lorentzian with the width $\Gamma = 2\pi \sum_{\ell} |V_{s\ell}|^2 \delta(E_s - E_{\ell})$ and the nonradiative lifetime $\tau = \hbar/\Gamma$. The experimental observation of a Lorentzian absorption lineshape due to internal conversion from the electronic origin (which precludes IVR) of some intravalence excitations of large isolated jet cooled molecules,⁵³⁻⁵⁷ e.g., the S_1 origin of azulene (Fig. 6) and the S_2 origin (Q_y band) of free base porphyrin (Fig. 7), as well as of the extravalence Rydberg excitations (principal quantum number $n = 3-5$) of benzene (Fig. 8), constitutes the victory of dynamics over spectroscopy for a highly congested bound level structure. The spectroscopic information (Table I) on ultrafast dynamics ($\tau = 3000-8$ fs) reveals that the time scale for internal conversion of high intravalence excitations of benzene and anthracene (8-20 fs) corresponds to the highest molecular vibrational frequencies $1500 \text{ cm}^{-1} - 3000 \text{ cm}^{-1}$. These energy-resolved data have to be supplemented by time-resolved information.

Fig. 6. The absorption spectrum of the 0-0 electronic origin of the $S_0 \rightarrow S_1$ of the isolated jet-cooled azulene molecule ($T_{\text{ROT}} = 20 \text{ K}$, $T_{\text{VIB}} = 30 \text{ K}$). The Lorentzian line broadening (fitted by a solid line) reflects intramolecular coupling and statistical limit $S_1(0-0) \rightarrow S_0^*$ relaxation in a bound level structure (reference 53).



3.2 Mode selectivity. The idea of mode selective unimolecular reactions is quite old, dating to Hinshelwood in the 1930s.^{59,60}

"In a molecule of moderate, but not too great, complexity it is not impossible that there may be several distinct modes of activation corresponding to particular divisions of energy among a limited number of vibrational (or rotational) degrees of freedom."^{59,60}

What is new is that current experimental and theoretical progress allows for the control of intramolecular and intermolecular dynamics via passive control of energy

Fig. 7. Absorption of the 0-0 electronic origins of the $S_0 \rightarrow S_2$ (Q_y band) of isolated jet-cooled free base porphyrin. The linewidth ($\Delta = 1.0 \text{ cm}^{-1}$) of the S_1 origin originated from rotational structure, while the Lorentzian line broadening (fitted by open circles) of the S_2 origin originates from intramolecular coupling and statistical limit $S_2(0-0) \rightarrow S_1^*$ relaxation in a bound level structure (reference 54).

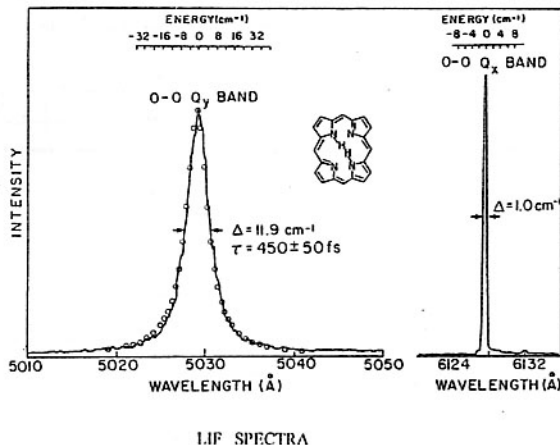
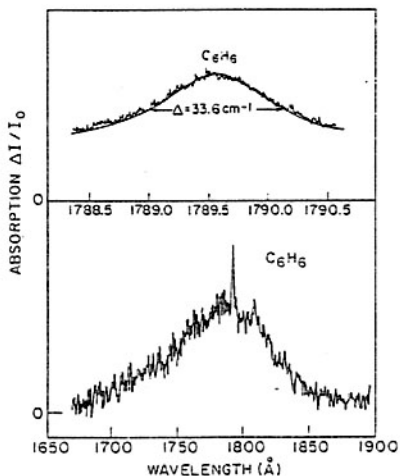


Fig. 8. Absorption spectrum of isolated jet-cooled benzene. Note the sharp feature, which corresponds to the $n=3$ Rydberg. The upper panel shows the lineshape analysis of the $Ru(3R_u)$ Rydberg, which is Lorentzian (fitted by a solid line) with a lifetime of $\tau = 154 \text{ fs}$ for C_6H_6 (and $\tau = 188 \text{ fs}$ for C_6D_6), exhibiting a small deuterium effect. Note that the Rydberg relaxation is considerably slower than the intravalence $\pi\pi^*$ excitation in the same energy domain (references 57, 58). Also note the lack of resonance Rydberg- $\pi\pi^*$ background interference effects (reference 57).



acquisition when the system evolves under its own Hamiltonian, as well as by active control of energy storage and disposal by the modification of the equations of motion by an external laser field.⁶¹ The characteristics of interstate coupling and intramolecular relaxation in a large isolated molecule can be more complex and interesting due to resonance effects, providing means for mode-selective dynamics.^{62,63} Mediated intersystem crossing from a S_1 vibronic state to the dense lowest triplet $\{T_1\}$ manifold can be induced by the sequential coupling via a sparse manifold $\{T_x\}$ of vibronic states corresponding to a higher triplet state. The theory

of mediated $S_1 \xrightarrow{V_{SO}} \{T_x^k\} \xrightarrow{V_{VIB}} \{T_1\}$ coupling and relaxation^{45,62,63} predicts the occurrence of resonances originating from $\{T_x\}$ - $\{T_1\}$ vibronic coupling (V_{VIB}), which mediate the decay of the S_1 doorway state induced by spin-orbit (V_{SO}) coupling. The perturbative weak coupling mediated intersystem crossing rate is^{45,62,63}

TABLE I
ELECTRONIC RELAXATION LIFETIMES IN ISOLATED JET-COOLED MOLECULES

MOLECULE	CHANNELS	τ (fs)
Azulene S_1	$S_1 \rightarrow S_0$ $\Delta E = 14400 \text{ cm}^{-1}$	800 ± 200
Phenanthrene S_2	$S_2 \rightarrow S_1$ $\Delta E = 4684 \text{ cm}^{-1}$	500 ± 100
Free-Base Porphyrin $S_2(Q_y)$	$S_2 \rightarrow S_1$ $\Delta E = 3540 \text{ cm}^{-1}$	450 ± 50
Zn-tetraphenyl Porphyrin	$S_2 \rightarrow S_1$	3200 ± 300
Benzene (H_6) Benzene (D_6) $n=3$ Rydberg	$3nR_y \rightarrow \{S_n\} \rightarrow S_0$	160 190
Benzene $S_3(^1E_{1u})$	$S_3 \rightarrow \{S_n\} \rightarrow S_0$	(20)
Anthracene $n = 3$ Rydberg	$3nR_y \rightarrow \{S_n\} \rightarrow$ $S_1 \rightarrow S_0$	180
Anthracene $S_3(^1B_{3u}^+)$	$S_3 \rightarrow S_1 \rightarrow S_0$	(7)

$$k(S_1) = \sum_k \frac{|V_k|^2 \gamma_k}{[E(S_1) - E(k)]^2 + \gamma_k^2}, \quad (3.1)$$

where $V_k = \langle S_1 | V_{SO} | T_x^k \rangle$ and $\gamma_k = 2\pi |\langle T_x^k | V_{VIB} | T_1 \rangle|^2 \rho$. Eq. (3.1) does not constitute a limit of the golden rule, but rather a superposition of sparsely spaced resonances. When the level structure of the $\{T_x\}$ - $\{T_1\}$ resonances is sparse, the decay rate is very sensitive to the energy gaps between the S_1 and T_x states. Accordingly, climbing up the vibrational levels in the S_1 manifold above its electronic origin will

result in a wide variation of their radiationless decay rates, exhibiting a marked mode selectivity of mediated intersystem crossing. Such dramatic vibrational mode-selective effects are revealed in the absolute fluorescence quantum yields from photoselected vibronic levels in the S_1 manifold of 9,10 dibromoanthracene,^{62,63} (Fig. 9), where the irregular variance of the nonradiative lifetimes spans about three orders of magnitude. These resonance effects for the decay of the S_1 state span the excess vibrational energy range $E_{\text{vib}} = 0\text{-}800\text{ cm}^{-1}$ above the electronic origin of the S_1 electronic manifold, while at higher E_{vib} mode selectivity is eroded due to intramolecular vibrational energy redistribution.

3.3 Towards chemistry. Long-range electron transfer (ET) in isolated supermolecules. ET reactions in chemistry, physics and biology have been almost exclusively explored in donor (D) - acceptor (A) systems embedded in a medium, e.g., solvent, glass or protein. The seminal Marcus theory of ET^{65,64} encompasses a broad spectrum of systems, e.g., ions in solution, supermolecules and biomolecules, with the solvent coupling playing a central role in the dynamics. Intramolecular ET can be realized as an interstate radiationless transition (section II), with the vibronic quasicontinuum acting as a dissipative channel.⁶⁵⁻⁶⁸ We have challenged the conventional wisdom regarding the dominating role of medium coupling in ET, proposed long-range ET which occurs in an isolated solvent-free supermolecule DBA (where B is a molecular bridge), and analyzed the structural and energetic constraints

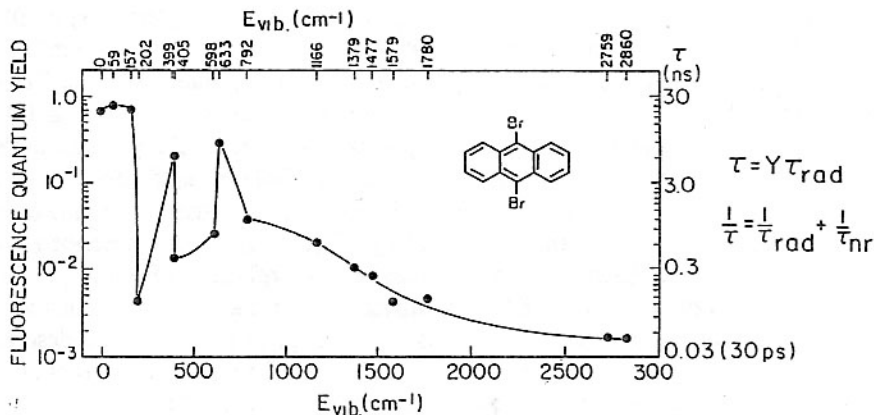


Fig. 9. Absolute fluorescence quantum yields (Y) and lifetimes (τ) of the photoselected vibronic level of jet-cooled 9,10 dibromoanthracene, which exhibit a marked mode selectivity in the vibrational energy range $0 \leq E_{\text{vib}} \leq 800\text{ cm}^{-1}$ above the electronic origin (reference 63).

for the occurrence of this radiationless transition.^{65,66} The order of the singlet electronic states of an isolated supermolecule exhibiting ET should involve the ground state $S_0(\text{DBA})$, the charge transfer state $S_1(\text{D}^+\text{BA}^-)$ and the localized excitation $S_2(\text{DBA}^*)$. A single vibronic level of $S_2(\text{DBA}^*)$ can act as a doorway state for internal conversion to the $S_1(\text{D}^+\text{BA}^-)$ quasicontinuum. The ladder diagrams for intramolecular ET are isomorphous to Fig. 2. It is gratifying that resonance Raman⁶⁹ and optical lineshape data⁷⁰ will allow for the quantification of these ladder diagrams. The realization of the molecular limit for ET⁶⁵⁻⁶⁸ in a (neutral) DBA requires an appropriate electronic level structure, being subjected to the structural-energetic constraints for the D-A (center-to-center) distance^{65,66} $R_{\text{DA}} \leq e^2/[I(\text{D})-E(\text{A})-E_{\infty}]$, i.e., $R_{\text{DA}} \leq 7\text{\AA}$, where $I(\text{D})$, $E(\text{A})$ and E_{∞} denote the ionization potential of D, the electron affinity of A and the electronic origin of the $(\text{DBA})^*$ transition. For small polaron transfer in D⁺BA and hole transfer in D⁺BA there are no constraints on R_{DA} .⁶⁵ The prediction for structural constraint in DBA was borne out by Verhoeven and Wegewijs⁷¹ for ET in isolated jet cooled rigid supermolecules, with D = dimethoxynaphthalene, A = dicarboxymethoxy ethylene or dicyanoethylene and B = norbornyl-like bridge with N bonds (denoted as DB_NA). $S_2(\text{DBA}^*) \rightarrow S_1(\text{D}^+\text{BA}^-)$ ET was observed for N = 3 with $R_{\text{DA}} = 5.8 \text{\AA}$, as expected. The theory provides dynamic rulers for ET in isolated supermolecules. The theory⁶⁵ also predicts the formation of giant D^+BA^- dipoles, with dipole moment $\leq 35\text{D}$ in molecular beams. Microscopic (state-selective) ET rates are given in the statistical limit in the form^{66,67} $k_s = (2\pi/\hbar)V^2\text{AFD}(E_s)$ in terms of a product of an electronic coupling (V) and the nuclear Franck-Condon overlap density $\text{AFD}(E_s)$. Isolated molecule ET rates exhibit the energy gap (ΔE) dependence (Fig. 10), with typical ET rates in the range $k_s = 10^{11}$ - $3 \times 10^{12} \text{ sec}^{-1}$ (with $V = 100 \text{ cm}^{-1}$) and $k_s = 10^{13}$ - $3 \times 10^{14} \text{ s}^{-1}$ (with $V = 1000 \text{ cm}^{-1}$) for charge separation from the electronic origin of the $S_2(\text{DBA}^*)$ state. For the DB_NA molecules (N = 3) $k_s \geq 10^{14} \text{ s}^{-1}$ (ref. 71) in accord with our estimate with $V \cong 1000 \text{ cm}^{-1}$. Another, more complex and interesting, isolated-molecule ET pertains to the DBA molecule with D = aniline and A = cyanonaphthalene, held together by a semirigid bridge^{72,73} (Fig. 11). Long-range ET in the extended structure, followed by electrostatically driven conformational folding (Fig. 11),^{72,73} was described⁶⁶ in terms of mediated nonradiative ET, whose rate is isomorphous to Eq. (3.1). This analysis builds a bridge between ET and intramolecular radiationless transitions. Unifying features of intramolecular dynamics can be applied to predict and describe other nonadiabatic processes, e.g., electronic energy transfer and spin-conversion in isolated supermolecules, opening up new areas of intramolecular chemistry.

3.4 Dynamics in intermediate level structure. Molecular quantum beats. Up to this point we were concerned with intramolecular dynamics in the statistical limit (Fig. 5). Of considerable interest is the isolated molecule intermediate level structure

Fig. 10. ET dynamics in isolated supermolecules. The energy gap ($-\Delta E$) dependence of the averaged Franck-Condon density (AFD) and the rate $k=(2\pi/\hbar)V^2$. AFD (with $V = 100 \text{ cm}^{-1}$) for the electronic origin. Calculations for a four intramolecular vibrational level system (ω/cm^{-1}) = (200,500,1200,1500) with couplings $S = (6,3,1,1)$. Note the exponential energy gap for charge separation at large $-\Delta E$.

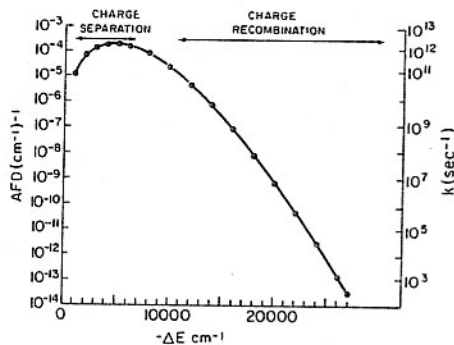
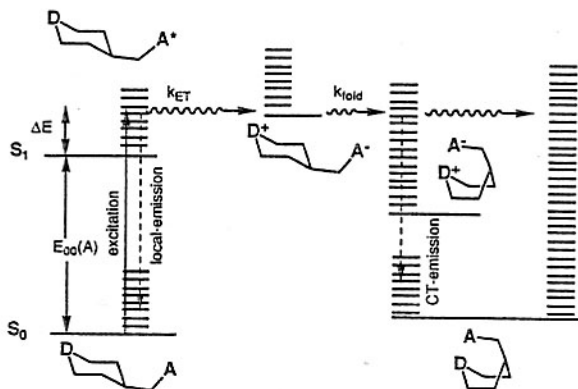


Fig. 11. Sequential long-range electron transfer and electrostatically driven conformational folding in an isolated semirigid DBA molecule. Isolated - molecule ET dynamics is described by a mediated intramolecular radiationless transition (reference 66).



characterized by $V\rho \gg 1$ and $\gamma\rho < 1$, where molecular eigenstates are distinct and weakly overlapping (Fig. 5). In such an intermediate level structure a wavepacket of molecular eigenstates can be coherently excited,^{25,26} reflecting the manifestations of the quantum mechanical superposition principle. A coherent excitation mode can be provided even by a ns laser pulse. Jortner and Berry²⁵ and Bixon, Dothan and Jortner²⁶ predicted that the time evolution of a molecular eigenstates wavepacket will exhibit interference effects in its radiative and nonradiative decay, which were referred to as molecular quantum beats. The time evolution manifested by the photon counting rate from the wavepacket is^{26,42,45,49,50}

$$I(t) = \sum_m |B_m|^2 \exp(-\gamma_m t) + \sum_m \sum_{m'} B_m^* B_{m'} \exp[i(E_m - E_{m'})t] \exp[-(\gamma_m + \gamma_{m'})t/2], \quad (3.2)$$

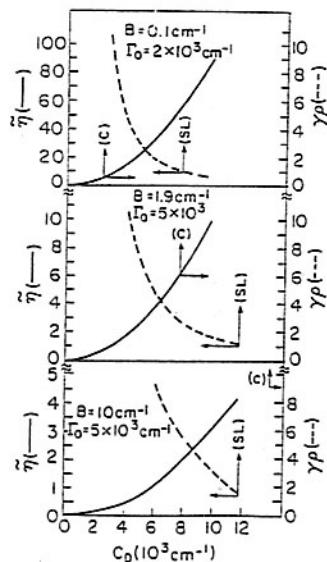
where $\{B_m\}$ are the excitation amplitudes containing information on the laser autocorrelation function, while the (real) energies $\{E_m\}$ and decay width $\{\gamma_m\}$ are specified by Eq. (2.8). In Eq. (3.2) the first sum corresponds to direct decay, while

the second sum represents the quantum beats. These interference effects provide spectroscopic and dynamic information, i.e., the frequencies $\{h/|E_m - E_m'|\}$ for energetics and the decay widths $\{(\gamma_m + \gamma_m')\}$ characterize the population decay of the independently decaying levels. This theory applies both to interstate and intrastate coupling. These predictions were subsequently confirmed by the experimental observation of molecular quantum beats from the intermediate level structure in the interstate S_1 - $\{T\}$ coupling of methyl glyoxal,⁷⁴ in the interstate S_1 - $\{T\}$ coupling of pyrazine^{27,28} and in the intrastate coupling between vibrational levels in the S_1 state of anthracene.⁷⁵ This novel dynamic-spectroscopic information on temporal quantum beats, originating from interstate and intrastate coupling, allowed for the direct observation of molecular eigenstates, making theoreticians' dreams come true. The origin of the exploration of molecular quantum beats is traced to the predictions^{25,26} and demonstrations^{27,28,74-77} of the dynamics of coherently (ns) excited wavepackets, while the advent of fs lasers resulted in rich information^{11,12,17-20} on vibrational coherence effects, which we shall allude to (section 6) in the context of cluster and condensed phase dynamics.

3.5 The electronic quasicontinuum. Up to this point we were concerned with intramolecular coupling and dynamics within a bound vibronic level structure of large molecules, with irreversible relaxation prevailing in a vibrational quasicontinuum, manifesting nuclear motion. Very high n ($=50-250$, where n is the principal quantum number) molecular Rydberg states correspond to microsystems (mean radius $\langle r \rangle = (3/2)n^2 a_0$, e.g., $r = 1 \mu$ for $n = 112$). They are characterized by a high density of electronic states in a bound level structure below the lowest ionization potential $IP(0)$ ($\rho(n) = n^3/2Ry$, e.g., $\rho(200) = 37 \text{ cm}^{-1}$), and by unique intramolecular nL - $n'L'$ (where L is the electron angular momentum) couplings which involve long-range Rydberg electron-core multipole and anisotropic polarizability interactions.^{78,79} A generalization and unification of the theory of coupling and dynamics for an electronic Rydberg manifold was provided,⁸⁰ establishing the conditions for strong coupling of a doorway state and the attainment of the statistical limit within an electronic quasicontinuum.⁸⁰ A generic example involves ultrahigh n, n' Rydbergs of a diatomic molecule with a doorway state $|n, L, N^+, M_N, N\rangle$ of low L ($= 0-3$) core-penetrating states converging to the ionization potential $I(N^+) = I(0) + BN^+(N^++1)$ (where B is the rotational constant, N^+ the core rotational quantum number and $\tilde{N} = \tilde{L} + \tilde{N}^+$), with decay widths given by the n^3 scaling law $\Gamma(n) = \Gamma_0/(n-\delta(L))^3$, where Γ_0 is the decay width parameter and $\delta(L)$ is the quantum defect. The electronic quasicontinuum $\{|n', L', N', M_N', N'\rangle\}$ converges to the lower ionization potential $I(0)$, while the Rydberg-core dipole coupling^{79,80} is $V = C_D(\lambda, \lambda', N^+, N^+, N)(nn')^{-3/2}$ with $\lambda = L - \delta(L)$. For coupling within the electronic manifold⁸⁰ the strong coupling limit ($V\rho(n') > 1$) is realized when $C_D/Ry > 2(8B(N^++1)/Ry)^{3/8}$, while the statistical limit ($\gamma\rho > 1$) is attained when $C_D/Ry <$

$(\Gamma_0/\pi R_y)^{1/2}$. From Fig. 12 we infer that the statistical limit will be realized in large polar molecules with $B \cong 0.1 \text{ cm}^{-1}$. For light molecules with large $B \cong 10 \text{ cm}^{-1}$ only strong coupling in the sparse mixed level structure can prevail, relating spectroscopy and dynamics. Another interesting aspect of the dynamics of Rydberg manifolds pertains to the coherent excitation and interrogation of a wavepacket of electronic states.⁷⁸

Fig. 12. Coupling and dynamics in the bound electronic quasicontinuum of Rydberg states. The strength C_D of the dipole coupling between $|n, N^+\rangle - \{|n', L', N^+\rangle$ Rydbergs (for different values of $B = 0.1-10 \text{ cm}^{-1}$) determines the coupling parameters $2\pi V^2 \rho^2$ and the linewidth parameters $\gamma \rho$. (C) denotes the onset of strong coupling for $C_D > C_D^{(C)}$. (SL) denotes the upper bound for $C_D < C_D^{(SL)}$ for the statistical limit.



3.6 Correlations in continua and quasicontinua. “Reactive” nonradiative processes of molecular (rotational, vibrational and electronic) predissociation and auto-ionization,⁸¹ which involve the decay of a metastable state(s) to a dissociation or ionization continuum, are known since the early days of molecular science.^{1,2} The theory of ‘nonreactive’ radiationless transitions in large isolated molecules, i.e., interstate coupling and electronic-vibrational relaxation (internal conversion and intersystem crossing) and in intrastate vibrational energy redistribution, involve dynamics in a bound vibronic (vibrational) Franck-Condon quasicontinuum (section 2). The theory of intramolecular dynamics has been extended (section 3.5) to explore coupling and relaxation within an electronic Rydberg quasicontinuum. The dissipative channels for intramolecular dynamics can be characterized in terms of the state specificity of the matrix elements of the Hamiltonian (\mathbf{H}), i.e., $V_{s\ell} = \langle s|\mathbf{H}|\ell \rangle$, for the coupling of the doorway states $|s\rangle, |s'\rangle, |s''\rangle\dots$, with the $\{|\ell\rangle\}$ states of the continuum or quasicontinuum. The state dependence of the couplings is quantified by the correlation parameters⁸²

INTRAMOLECULAR DYNAMICS

ISOLATED MOLECULES



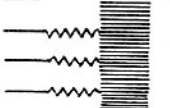
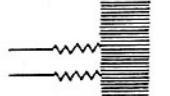
RELAXATION PROCESS	DISSIPATIVE CHANNEL
AUTOIONIZATION (1930-)	IONIZATION CONTINUUM "SMOOTH" COUPLING 
PREDISSOCIATION (1928-)	DISSOCIATION CONTINUUM "SMOOTH" COUPLING 
RADIATIONLESS TRANSITIONS BOUND LEVEL STRUCTURE (1968-)	VIBRONIC FRANCK-CONDON QUASICONTINUUM "BUMPY" WEAKLY CORRELATED COUPLING 
ELECTRONIC RELAXATION ULTRAHIGH RYDBERGS (1996-)	ELECTRONIC QUASICONTINUUM "SMOOTH" COUPLING 

Fig. 13

$$\eta_{ss'} = \langle V_{s\ell} V_{\ell s'} \rangle / [\langle V_{s\ell}^2 \rangle \langle V_{s'\ell}^2 \rangle]^{1/2} , \quad (3.3)$$

where $\langle \rangle$ denotes averaged products over the energy range which includes E_s and $E_{s'}$. The continua and quasicontinua can be segregated into (Fig. 13): (i) 'Smooth' decay channels, involving slow energy dependence (E_ℓ) of $V_{s\ell}$, with $\eta_{ss'} = 1$ for $s \neq s'$, i.e., dissociative and ionizative continua and the electronic quasicontinuum, and (ii) 'nonsmooth' decay channels, where $V_{s\ell}$ exhibits a large

and irregular energy (E_ℓ) variation, $\eta_{ss} \ll 1$; $s \neq s'$, i.e., the vibronic (vibrational) Franck-Condon quasicontinuum. The distinction between 'smooth' and 'nonsmooth' channels does not affect the level structure and dynamics of molecular eigenstates which have their parentage in a single doorway state coupled to a single quasicontinuum. This distinction is of central importance for interference effects between several doorway states, which exhibit a profound influence on femtosecond intramolecular dynamics in electronically-vibrationally excited wavepackets of states of large isolated molecules and in the condensed phase. The correlation parameters η_{ss} affect vibrational coherence in nonradiative dynamics⁸² and determine the upper temporal limits for relaxation.⁸³ The nature of sequential dynamics in a system consisting of doorway state(s) in resonance coupling to consecutive quasicontinua or continua is dominated by these correlations (section 7).⁸³

4. How fast is ultrafast?

In the context of ultrafast chemical and biophysical dynamics it is appropriate to inquire: how fast is ultrafast? This question attracts different answers in different areas of science (Fig. 14). In the realm of chemical, i.e., molecular, cluster, condensed phase and biological dynamics, ultrafast relaxation can prevail on the time scale of nuclear motion. The preceding discussion of intramolecular dynamics within a vibrational manifold raises the central issue regarding the upper limit for the rates k of several classes of molecular ultrafast processes: (i) 'nonreactive' relaxation in a bound level structure, (ii) 'reactive' processes, e.g., electronic or vibrational predissociation, and (iii) direct dissociation and Coulomb explosion. These temporal upper limits are determined by the time scale of nuclear motion, which have to be quantified.

For intramolecular relaxation processes involving a 'smooth' correlated ($\eta_{ss} \cong 1$), dissipative channel, the temporal constraints on the dynamics can be inferred from the theory of overlapping resonances,^{84,85} which sets an upper limit on k . For the population decay of a set of equally spaced (nearest neighbor separation of ω) resonances (of widths $\Gamma = 2\pi V^2 \rho$ for an isolated resonance), interference effects set in when $\Gamma \sim \omega$. The intramolecular relaxation rate is $k = (\Gamma/\hbar) / [1 + (\pi\Gamma/\omega)]$. The rate exhibits a transition from $k = (\Gamma/\hbar)$ for an isolated resonance ($\Gamma \ll \omega$) to $k = \omega/h$ for overlapping resonances ($\Gamma \gg \omega$). The overlapping resonances domain provides an upper limit for the nonradiative rates, i.e., $k \leq \omega/h$, which is determined by the level spacing, i.e., the vibrational frequency (time scale $t \sim k^{-1} \sim 10$ -1000 fs for $\omega = 3000$ -30 cm^{-1}). This situation prevails for intramolecular dynamics in a 'smooth' nuclear continuum, i.e., electronic and vibrational predissociation. For dynamics in the 'smooth' electronic Rydberg quasicontinuum the upper limit for the rate is $k \leq 2Ry/n^3h$ (i.e., k for $n = 50$ being in the (ps)⁻¹ domain).

For the decay of weakly correlated ($\eta_{ss} \ll 1$) overlapping resonances into a 'nonsmooth' Franck-Condon vibrational quasicontinuum, interference effects are expected to be much less pronounced than for the case of a 'smooth' channel. This is experimentally manifested in the related context of the lack of interference effects, i.e., Fano antiresonances in the absorption spectra of Rydberg states which overlap $\pi\pi^*$ intravalence excitations in large aromatic molecules (Fig. 8). Model calculations of correlation parameters η_{ss} for a doorway state in the vicinity of the electronic origin are considerably lower than unity, with their highest values falling in the range $|\eta_{ss}| = 0.4 - 0.2$ for a small number of s, s' pairs differing only by a single vibrational quantum number, while for multimode s, s' changes very low values of $|\eta_{ss}| < 0.1$ are exhibited.⁸² These propensity rules⁸² imply the existence of weak correlations within the Franck-Condon vibrational quasicontinuum, resulting in a partial erosion of resonance interference effects, in some analogy with random coupling models for intramolecular coupling and dynamics,⁸⁶⁻⁸⁸ where interference effects are completely eroded. Ultrafast intramolecular radiationless transition rates in a bound level structure of overlapping resonances into the Franck-Condon quasicontinuum are expected not to be strictly limited by the level spacing, but rather the temporal upper limit $k \propto V^2 \geq \omega/\hbar$ can be realized. Indeed, some of the ultrafast (~ 10 fs) relaxation times of intravalence excitations of isolated aromatic molecules (Table I) exceed most of the intramolecular frequencies. Such temporal records may be achieved for 'nonreactive' radiationless transition in large molecules and for nonadiabatic processes in liquids, solids and proteins, providing (sections 6 and 7) a unification of intramolecular and condensed phase ultrafast dynamics.

For direct dissociation in molecular systems the dynamics involves the sliding on a repulsive potential surface.^{13,14} The characteristic time for dissociation is described in terms of a classical mechanical model of Zewail and his colleagues^{13,14}

$$\tau_c = \int_{R_0}^R \frac{dR'}{v(R')} \quad , \quad (4.1)$$

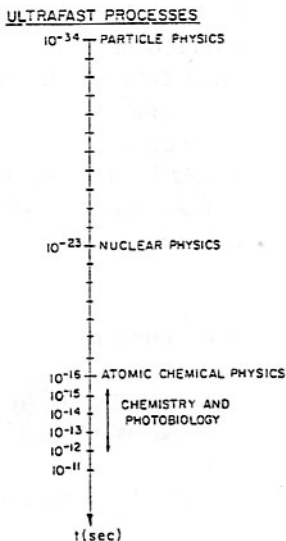
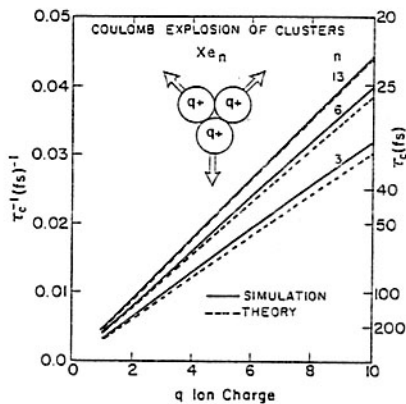


Fig. 14

where $v(R')$ is the velocity at R' . A more complete and sophisticated treatment of this important problem was provided,⁸⁹ but Eq. (4.1) captures the essential features of the dynamics. The typical time scale for direct dissociation is $\tau_c \cong 100$ fs.

An ultrafast excitation leading to the localization of energy in polyatomic molecules or clusters can be achieved by a Coulomb explosion.^{15,16,90} This ultrafast process is characterized by site selective energy acquisition in conjunction with bond-specific energy disposal. The mechanical model, Eq. (4.1), for the separation of two positive ions of charges $q = 1$ gives^{15,90} $\tau_c \cong (\ell / 2v_c) \ln(4\langle R \rangle / \ell_c)$, where $v_c = (2E/\mu)^{1/2}$ is the terminal speed, $\ell_c = (e^2/E)$ is the terminal length, and E is the terminal kinetic energy. This simple argument results in $\tau_c \cong 10$ fs. The time scale for Coulomb explosion can be shorter by about one order of magnitude than the corresponding time scale for direct molecular dissociation.¹⁵ The theory of Coulomb explosion was developed for clusters.⁹⁰ The time scales obtained from the classical model for the explosion of a $(Xe^{q+})_n$ cluster reveal that $\tau_c^{-1} \propto q$, being borne out by molecular dynamics simulations⁸² (Fig. 15). The utilization of the ultrafast fs "chemical clock" of Coulomb explosion of molecules,¹⁵ surface states¹⁵ and clusters^{16,90} precludes IVR and shows potential application for selective chemistry.

Fig. 15. Coulomb explosion dynamics of $(Xe^{q+})_n$ clusters. The $\tau_c \propto q$ dependence of the reciprocal Coulomb explosion time is in accord with the classical picture based on Eq. (4.1).



5. Cluster dynamics. Large finite systems

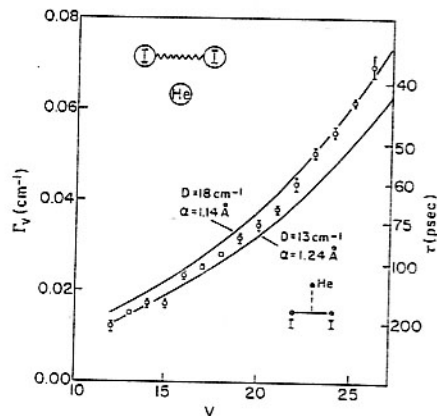
We proceed from the world of intramolecular dynamics to cluster dynamics. The conceptual framework for modern cluster chemistry originated from structural considerations for close packing of hard spheres⁹¹ and from the exploration of the dynamics of van der Waals molecules⁹² containing rare-gas atoms. Smalley, Levy and Wharton^{9,10} discovered weakly bound rare-gas atom-halogen molecule van der Waals clusters, i.e., $He \cdot I_2$, initiating the experimental exploration of cluster electronic-vibrational spectroscopy and dynamics. The theory of vibrational

predissociation (VP) of clusters was advanced by Beswick and Jortner⁹³⁻⁹⁵ and applied to vibrational-translational intracluster energy transfer in the HeI₂ (Fig. 16). The VP linewidth (i.e., $\hbar(\text{rate})$) of AB•R can be semiquantitatively described by^{93,94,52}

$$\Gamma = \hbar \nu \exp[-\pi d(2\mu\epsilon/\hbar)^{1/2}] , \quad (5.1)$$

where ν is the effective (AB-R) vibrational frequency, d the range of the interaction, μ the effective mass and ϵ the kinetic energy of the fragments. The theory⁹³⁻⁹⁵ establishes an energy gap law ($\ln\Gamma \propto \epsilon^{1/2}$) for VP, while Eq. (5.1) is isomorphous to a tunneling formula. The Beswick-Jortner theory⁹³⁻⁹⁵ was successfully applied for real-time vibrational predissociation of clusters.⁹⁶ VP of these van der Waals clusters exhibits nonstatistical dynamics, reflecting a slow intramolecular energy flow due to the considerable frequency mismatch between the (high frequency) molecular bond and the (low frequency) van der Waals bonds, which provides a bottleneck to vibrational energy transfer.^{15,52,95}

Fig. 16. Vibrational predissociation linewidths (Γ_v) and lifetimes (τ) of the He•I₂ cluster for photoselected vibrational (ν) states of I₂, calculated (solid lines) by Beswick and Jortner (1978). D represents the cluster dissociation energy. The experimental data (open points) of Smalley, Wharton and Levy (refs. 9,10) are well accounted for.



Clusters, i.e., finite aggregates containing 2-10⁹ constituents, provide novel insight into the dynamics of systems with finite density of states, where separation of time scales can be realized.⁹⁷ A key concept for the quantification of the unique characteristics of clusters pertains to size effects. These involve the evolution of structural, thermodynamic, electronic, energetic, electrodynamic and dynamic features of finite systems with increasing the cluster size. Dynamic cluster size effects were explored on the theoretical front by modelling and by molecular dynamics simulations.⁹⁷⁻⁹⁹ Some dynamic effects ((2) and (4) above) can be quantified by cluster size equations due to cluster packing, while others ((1) and (3)

above) provide rich information of intracluster vibrational energy flow and structural changes.

(1) The 'transition' from molecular-type dissociative dynamics in small clusters to condensed-matter type nonreactive vibrational relaxation in large clusters, manifests the bridging between molecular and condensed phase nuclear dynamics.¹⁰⁰

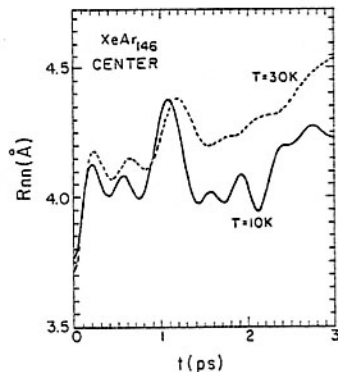
(2) Collective vibrational modes. Of interest are interior, collective, compression modes of planets, of nuclei and of clusters.^{98,99} Collective nuclear modes of atomic clusters (He_n , Ar_n) were treated^{98,99} in terms of the excitation of a liquid drop with the frequency $\hbar \omega_B(n) = \hbar \omega_B(\infty) + (\pi \hbar u/R_0)n^{1/3}$, where $\omega_B(\infty)$ is the surface mode of the corresponding solid, u the velocity of sound and R_0 the constituent radius. These cluster collective modes were experimentally observed¹⁰¹ with their frequency being well accounted for in terms of the dynamic cluster size equation. Complementary to the energetics of these collective modes, their dynamics is interesting. The damping of the collective motion via the coupling of a 'giant resonance' to non-coherent vibrational modes, constitutes a theoretical and experimental challenge.

(3) Bubble dynamics. The dynamics of large local configurational charge are induced by an extravalence excitation of a probe atom (e.g., $^1\text{S}_0 \rightarrow ^3\text{P}_1$ excitation of Xe) or molecule (e.g., Rydberg excitation of NO) in a rare-gas cluster. Molecular dynamics simulations of the dynamics of configurational nuclear relaxation around the $^3\text{P}_1$ excitation of Xe located in the central site in XeAr_n clusters (Fig. 17) reveals:⁹⁸ (i) Large configurational dilation, i.e., 'bubble' formation on the time scale of $t_B \sim 200\text{-}300$ fs. (ii) t_B marking the time scale for ultrafast energy transfer. (iii) Multimodal time evolution, with slower time scales of 1-5 ps. (iv) Marked impact vibrational coherence excitation. This vibrational coherence (Fig. 17) characterizes the collective vibrations around the excited probe atom with a long time scale for dephasing of 1-5 ps, considerably exceeding the time scale for initial configurational relaxation. The local configurational dilation ($\Delta R_{nn} \cong 0.7\text{-}0.8\text{\AA}$) around an extravalence excitation in Ar_n clusters (and in the condensed phase) can be greatly spatially amplified for excess electron localization in liquid He, where the equilibrium electron bubble radius $R_b = 17\text{\AA}$ (at $P = 0$)¹⁰³ is huge. The dynamics of excess electron localization in liquid He on a time scale of $\tau_b \sim 8$ ps at 0.4 K rests on a quantum mechanical description of the electron in conjunction with a hydrodynamic model including energy dissipation for the liquid.¹⁰³ The fluid dynamics is described¹⁰³ in analogy to molecular dissociation, Eq. (4.1).

(4) Ultrafast energy acquisition via high-energy cluster-wall collisions. High-energy impact of atomic or molecular cluster ions (of sizes 10-1000 constituents, with velocities up to $V \sim 20\text{ km s}^{-1}$ and kinetic energies up to ~ 100 eV per particle) on insulator, semiconductor or metal surfaces, produces a new medium of extremely high density (up to ~ 4 times the standard density), high temperature (up to $\sim 10^5$ K) and high energy density (up to 10^2 eV per particle), which is temporarily generated during the propagation of a microshock wave within the cluster. The energy

acquisition process for cluster-wall high-energy collision was characterized^{98,102} by the residence time $\tau_c = R_c/v$, with the cluster radius $R_c = R_0 n^{1/3}$. τ_c is given by the width of the time-dependent cluster potential energy curve, providing the time scale for the intracluster microshock wave propagation, which is described by a dynamic cluster size equation $[\tau_c(n)]^{-1} = (v/R_0)n^{-1/3}$, with time scales of $\tau_c = 10$ -500 fs.¹⁰² Chemical applications, e.g., cluster impact dissociation of a probe diatomic molecule, were simulated.¹⁰² The dissociation process is limited by the vibrational period of the molecule. Cluster impact dynamics opens up a new research area of thermal femtosecond chemistry.

Fig. 17. The time evolution of the average Xe-Ar distance R_{nn} of Xe(³P₁) at the central site in XeAr₁₄₆. $T = 10$ K, 30K mark the equilibrium cluster temperature prior to excitation. Configurational dilation is manifested by the increase of R_{nn} on the time scale of ~ 200 fsec. Note the impact vibrational coherence manifested by oscillations in R_{nn} .



6. Nonradiative relaxation in the condensed phase

The central idea in the realm of condensed phase dynamics was advanced in 1949 by Franck in a private communication to Libby,¹⁰⁴ asserting that the Franck-Condon principle is applicable for thermal ET processes in solution. Subsequently, the pioneering studies of Kubo on electron-hole recombination,⁵ of Marcus on ET⁶ and of Förster on electronic energy transfer,⁷ laid the foundations for the theory of radiationless processes in the condensed phase and in protein medium (Table II). The isomorphism between condensed phase and intramolecular radiationless transitions (sections 2 and 3) in the context of ET in solution was addressed by Kestner, Logan and Jortner¹⁰⁵ within the incorporation of quantum effects in ET theory:

“The general features...of thermal electron transfer processes bear a close resemblance to the theoretical description of a wide class of molecular relaxation processes such as nonradiative intramolecular relaxation in the statistical limit.”¹⁰⁵

Indeed, both condensed phase and intramolecular radiationless transitions are induced by the coupling of doorway state(s) to a vibronic quasicontinuum. A unified

conceptual framework for all these condensed phase radiationless transitions (Table II) considers population relaxation between two potential surfaces of the entire system corresponding to distinct zero-order electronic configurations with energy conservation being insured by absorption and emission of medium phonons and intramolecular vibrations. For a nonradiative process from a reactant doorway vibronic state $|s\rangle$ to the vibronic manifold $\{|\alpha\rangle\}$ of product states quasidegenerate with it the microscopic rate is given by the golden rule expression

$$k_s = (2\pi/\hbar)|V|^2 F_s, \quad (6.1)$$

where the Franck-Condon densities are

$$F_s = \sum_{\alpha} |\langle s|\alpha\rangle|^2 \delta(E_s - E_{\alpha}) \quad (6.2)$$

The electronic couplings V are specified in Table II.

We proceed to consider the broad field of ET. A basic assumption underlying the microscopic description of the rate k of such nonadiabatic processes in terms of the microscopic rates (6.1) is the insensitivity of the ET dynamics to the medium dynamics, which can be realized under one of the following conditions: (i) The common situation of fast medium vibrational dynamics, which allows the separation of time scales between the fast medium relaxation and slow ET, with the microscopic ET rate constants constituting the rate determining step. Under these circumstances the rate k is expressed^{105,106} in terms of a thermal average $k = \sum_s P_s k_s$, where P_s is the thermal population of level $|s\rangle$, with k being given by a finite temperature generalization of Eq. (2.5). (ii) The microscopic rates depend weakly on the initial vibronic manifold. Under these circumstances $k \cong k_s$ (for the relevant doorway states). Such a state of affairs prevails for activationless ET, where the potential surfaces cross in the vicinity of the minimum of the initial state, which pertains to the optimization of the ET rate. Weak state specific k_s also prevails for inverted region ET where high frequency vibrations of the D and A centers result in intramolecular vibrational excitation induced by ET.¹⁰⁶

Ultrafast femtosecond ET reactions in condensed phase are expected to correspond to activationless ET. Such reactions are not limited by solvent dynamics,¹⁰⁷ which was traditionally specified by the solvent relaxation time $\langle\tau\rangle$ induced by a constant charge, with the solvent adiabaticity parameters $\kappa = 4\pi|V|^2\langle\tau\rangle/\hbar\lambda$. For $\kappa \gg 1$ an activationless ET would apparently be characterized by $k \cong \langle\tau\rangle^{-1}$, setting an upper limit on the rate. This expectation was violated¹⁰⁷ by several ET experiments with ET rates in the range $(100 \text{ fs})^{-1} - (1000 \text{ fs})^{-1}$, which resulted in $k\langle\tau\rangle = 50-100$. The origin of the failure of the theory of solvent controlled ET was traced to the weak excess energy dependence of the microscopic rates¹⁰⁷ for the activationless

(and the inverted region) process, which implies that ET cannot be described by diffusion towards the intersection of the potential energy surfaces at the minimum of the initial DA surface. Rather, the depletion dynamics of the DA manifold occurs from an entire manifold of doorway states. ET fs dynamics is limited by the electronic coupling and the nuclear Franck-Condon factors, in analogy to intramolecular dynamics.

TABLE II
INTERMOLECULAR NONRADIATIVE PROCESSES IN CONDENSED PHASE

Process	Electronic States		V Electronic Coupling
Electronic transfer in solids, liquids and biological systems	$DA \rightarrow D^+A^-$ D = electron donor A = electron acceptor	J. Franck R.A. Marcus	Two-center Coulomb + exchange
Small polaron	$A^+A \rightarrow AA^+$ A = neutral molecule A^- = negative ion	T. Holstein	Two-center one-electron Coulomb and exchange
Electron-hole recombination in semiconductors	$D^+ k\rangle \rightarrow D^+ b\rangle$ $ k\rangle$ = free electron $ b\rangle$ = electron bound to D^+ D^+ = positive ion	R. Kubo Y. Toyozawa	Nuclear momentum
Electronic energy transfer in solids, glasses, and liquids	$D^+A \rightarrow DA^+$ D = energy donor A = energy acceptor	T. Förster D. Dexter	Intermolecular electrostatic interaction dipole-dipole monopole-monopole, also electron exchange
High-spin low-spin interconversion in transition metal compounds	$M(S1) \rightarrow M(S2)$	M. Bixon	Spin-orbit
Group transfer in hemoglobin	$Fe(S=2) + CO \rightarrow Fe(S=2) \cdot CO$	H. Frauenfelder	Spin-orbit

The observation of a wealth of vibrational coherence effects for reactants and products in condensed phase chemical and biophysical systems¹⁸⁻²⁰ transcends the description of nonradiative, nonadiabatic dynamics in terms of Eqs. (6.1) and (6.2). In particular, the weak, but finite, correlation parameters $\eta_{ss'}$ (section 3.6) are crucial in determining vibrational coherence in reactant and in product states. An analysis⁸² of the time evolution of an initially excited coherent wavepacket of doorway states $\Psi(0) = \sum_s A_s(0)|s\rangle$ reveals that the interstate nonradiative dynamics is determined

by the microscopic rates $\{k_s\}$ and by the off-diagonal matrix elements of the decay matrix $\Gamma_{ss'} = \eta_{ss'}(\hbar/2)(k_s k_{s'})^{1/2}$, with $\eta_{ss'}$ defined by Eq. (3.3). The time dependence of the nonradiative decay probability $P(t)$ (for the relevant limit $\Gamma_{ss'} < |E_s - E_{s'}|$) is⁸²

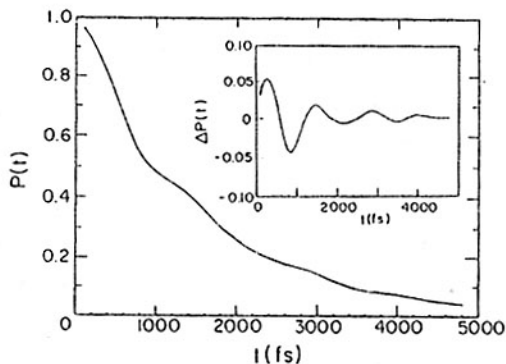
$$P(t) = \sum_s |A_s(0)|^2 \exp(-k_s t) + \sum_{\{s\} \neq \{s'\}} A_s(0) A_{s'}(0) \left[\frac{i\hbar \eta_{ss'} (k_s k_{s'})^{1/2}}{2(E_s - E_{s'})} \right] \exp[i(E_s - E_{s'})t/\hbar] \exp[-(k_s + k_{s'})t/2] \quad (6.3)$$

The manifestation of quantum beats terms in $P(t)$ is determined by the spectroscopic, energetic and dynamic properties of the doorway states which pertain to: (i) large preparation amplitudes $\{A_s(0)\}$, (ii) periods $T_p = \hbar/|E_s - E_{s'}|$ of quantum beats, (iii) modulation amplitudes determined by $\Gamma_{ss'}/|E_s - E_{s'}|$ and (iv) sufficiently large correlation parameters $\eta_{ss'}$. While features (i) and (ii) provide the signature of the laser excitation conditions, features (iii) and (iv) constitute the features of nonadiabatic nonradiative coupling and dynamics, providing the distinction between the experimental aspects of wavepacket preparation and the intrinsic manifestations of interstate dynamics. Raising the issue of how coherent excitation of a wave packet of doorway states modifies nonadiabatic dynamics, we assert that indeed the temporal modulation amplitudes in $P(t)$ are determined by condensed phase dynamic parameters $\eta_{ss'}$, however, the overall influence on the modulation of $P(t)$ is small (Fig. 18). On the other hand, the amplitudes of the pronounced quantum beats in the photon counting rate $I(t)$ from the excited wavepacket do not provide information on the nonradiative interstate dynamics, just reflecting radiative interference effects.⁸² Vibrational coherence effects in the electronically excited bacteriochlorophyll dimer (${}^1P^*$) of the bacterial photosynthetic reaction center (RC)¹⁹ interrogated by the (spontaneous and induced) fluorescence decay $I(t)$ just provide spectroscopic information on features (i) and (ii) above, but not on the charge separation dynamics.

7. Primary charge separation in photosynthesis.

The conversion of solar energy into chemical energy in reaction centers (RC) of

Fig. 18. Temporal vibrational coherence in nonadiabatic dynamics, showing the non-radiative decay probability $P(t)$ of the reactants manifold to a vibronic quasicontinuum. Data for a four-mode Franck-Condon system with frequencies $\omega/\text{cm}^{-1} = (117, 75, 35, 27)$, coupling parameters $S = (1.0, 1.1, 1.2, 3.0)$, energy gap $\Delta E = 500 \text{ cm}^{-1}$ and electronic coupling $V = 20 \text{ cm}^{-1}$. The initial wavepacket consists of the seven lowest states in the doorway manifold with the amplitudes given by the appropriate vibrational overlap integrals from the ground electronic-vibrational state. The insert shows the time dependence of $\Delta P(t) = P(t) - \text{Av}[P(t)]$, reflecting low amplitudes of the quantum beats.



photosynthetic bacteria and plants proceeds via a sequence of well organized, highly efficient, directional and specific ET steps between prosthetic groups across the membrane protein. The experimental exploration of ultrafast biophysical dynamics in a protein medium started 20 years ago for ET in the bacterial photosynthetic RC.^{108,109} These pioneering studies of Rentzepis et al¹⁰⁸ and Windsor et al¹⁰⁹ determined the time scales for the oxidation of the special pair P ($\tau < 10$ ps) and for the reduction of the quinone Q ($\tau \cong 200$ ps). The unification of the theory of ET in solution and in biophysical systems, was accomplished at that time.¹¹⁰ The central ingredients of this general theory involve the quantum description of the electronic coupling together with the intramolecular high frequency nuclear motion, in conjunction with the classical Marcus description⁶ of medium coupling. The ET rates (constrained by insensitivity to medium dynamics)¹⁰⁷ were given¹¹⁰ in terms of the nonadiabatic multiphonon theory (section 6) in the form $k = (2\pi/\hbar)|V|^2F$. V is the electronic coupling which is due to direct (many electron) D-A exchange or to mediated D-B-A superexchange (via the off-resonance states of the bridge B), being determined by D-A separation, orientation and/or bridging, manifesting structural control of ET. F is the thermally averaged nuclear Franck-Condon factor, which is determined by the coupling of medium modes and of high-frequency intramolecular modes and by the D^+A -DA energetics, manifesting medium and intramolecular control of ET. Prior to the availability of structural information on the RC, two significant results of ET theory were obtained for ET in the RC. Firstly, the optimization of F and of the ET rate for activationless ET was advanced,^{111,112} with $k \cong (4\pi\lambda k_B T)^{-1/2} \exp(-S)$ (where S is the intramolecular coupling), to account for the

surprisingly weak non-Arrhenius type $k \propto T^{-1/2}$ temperature dependence of the rates of $^1P^*$ oxidation and of the quinone reduction.¹⁰⁸ Secondly, the exponential dependence $V \propto \exp(-\alpha R)$ of the electronic coupling on the D-A separation (R), i.e., $k \propto \exp(-2\alpha R)$, was invoked^{111,112} for a rough estimate of the (center-to-center) distances between P and the primary acceptor ($R \sim 10 \text{ \AA}$) and between the bacteriochlorophyll (H) and Q ($R \sim 14 \text{ \AA}$), which provided some preliminary information on structure-dynamics relations. The seminal determination of the structure of the bacterial photosynthetic (RC) in 1985¹¹³ led to a metamorphosis in the study of photosynthesis. Nevertheless, the basic issues which pertain to the dynamics of the primary charge separation, are not yet elucidated. The major limitations in the understanding of this central energy conversion process in photobiology is that it requires information on the energetics, electronic interactions, and (intermolecular and intramolecular) nuclear dynamics, which cannot be inferred from the structural data in the ground electronic state. The outstanding problems in the understanding of the primary charge separation from $^1P^*$ to the bacteriochlorophyll (H) are:

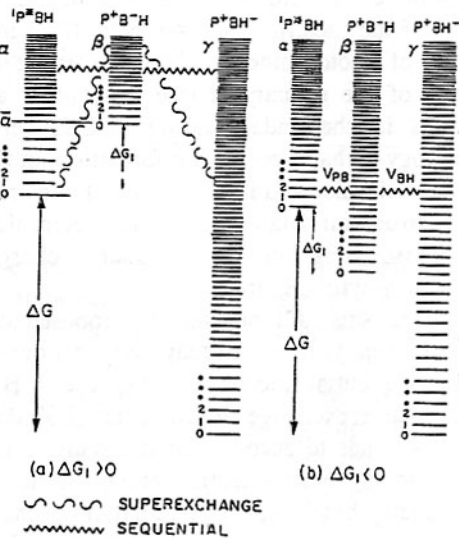
(A) Mechanisms. All mechanisms proposed attribute a special role to the accessory bacteriochlorophyll B, which may involve a one-step superexchange mechanism,¹¹⁴ a two-step sequential mechanism via the P^+B^-H intermediate,¹¹⁵ or the parallel sequential-superexchange mechanism (PSSM).^{116,117} The mechanistic issue is central, as it has to account for the stability of the photosynthetic apparatus with respect to mutagenesis, chemical and environmental perturbations.

(B) Symmetry breaking. The remarkable unidirectionality of the primary charge separation across a single (A) branch of the RC¹¹⁴ is attributed to the cumulative contributions of the electronic coupling and of the nuclear Franck-Condon factors (originating from the $^1P^* - P^+B^-H$ energetics) with both classes of effects reinforcing the branching ratio for ET across the A branch. The reason for the structural redundancy of the RC constitutes a central open question.

Our description^{116,117} of primary ET in the RC rests on the theory of dynamics in a Frank-Condon system with two quasicontinua⁸³ (Fig. 19). For a single vibronic doorway state $^1P^*BH|\alpha\rangle$ with off-resonance $^1P^*BH|\alpha\rangle - P^+B^-H\{|\beta\rangle\}$ coupling ($\Delta G_1 > 0$), a unistep superexchange mechanism prevails for $\alpha < \bar{\alpha}$. For resonance $^1P^*BH|\alpha\rangle - P^+B^-H\{|\beta\rangle\}$ coupling ($\Delta G_1 < 0$) of a single doorway state $|\alpha\rangle$ a two-step sequential mechanism is manifested for all $|\alpha\rangle$, being induced by phase erosion due to weakly correlated ($\eta_{\beta\beta} \ll 1$, according to section 3.6), $P^+B^-H\{|\beta\rangle\} - P^+B^-H\{|\gamma\rangle\}$ interquasicontinua coupling.⁸³ Simulations of the ET dynamics based on the time evolution of wavepackets of doorway states in a multimode system (Fig. 19), in conjunction with quantum mechanical calculations of the microscopic rates reveals the 'transition' from the sequential to the superexchange domain for ET from a single doorway state (Fig. 20), establishing the energetic control of ET. State selective ET dynamics for a single doorway state $|\alpha\rangle$ is either sequential or

superexchange type. For a system characterized by a small energy gap $\Delta G_1 (> 0)$ at a finite temperature, the thermally averaged rate for a microcanonical ensemble of initial ${}^1P^*BH\{|\alpha\rangle\}$ doorway states will result in a superposition of both sequential and superexchange mechanisms (for different vibronic states), whose branching ratio will be temperature dependent, providing the conceptual basis for the PSSM.^{116,117}

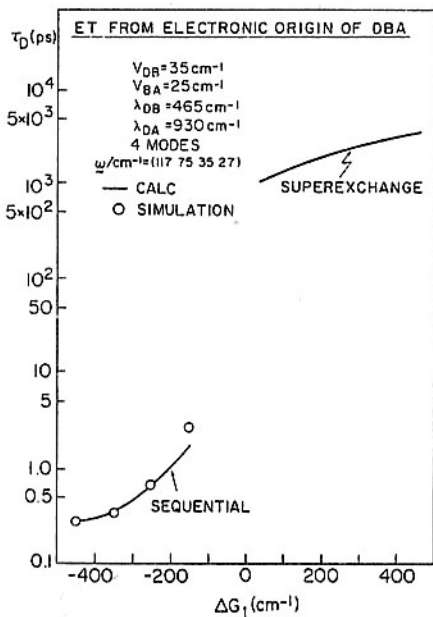
Fig. 19. Level structure for the primary charge separation in native, genetically engineered and chemically modified photosynthetic RC. The decay of the electronic origin of the doorway ${}^1P^*BH$ manifold ($|\alpha\rangle = |0\rangle$) corresponds to sequential dynamics (involving the chemical intermediate P^+B^-H) for resonance coupling ($\Delta G_1 < 0$) and to uni-step superexchange dynamics for off-resonance ($\Delta G_1 > 0$) coupling.



Primary ET in the RC occurs within an energetically congested electronic level structure with small energy gaps, whereupon the central energetic parameter ΔG_1 (Fig. 19) cannot be inferred from a-priori theory and simulation. The energetic control of the ET mechanism (Fig. 20) implies that for the native RC of photosynthetic bacteria at room temperature ($\Delta G_1 = -500 \pm 160 \text{ cm}^{-1}$ ¹¹⁷), the primary ET is dominated by the sequential mechanism, in accord with time-resolved experiments. Structure invariant mutagenic and chemical engineering of the RC which modifies ΔG_1 provides a powerful method for the exploration of dynamic-energetic relations (e.g., Fig. 20). Single-site mutants, which modify the energetics of ${}^1P^*$ ($\Delta G_1 = -1200 - 100 \text{ cm}^{-1}$) preserve the sequential mechanism at room temperature (Fig. 21), while at low temperatures the superexchange route (expressed by the superexchange branching ratio F_{SUP}) will contribute for higher ΔG_1 (e.g., for $\Delta G_1 = 100 \text{ cm}^{-1}$ $F_{\text{SUP}} = 0.5$ at $T = 20 \text{ K}$).¹¹⁷ For triple hydrogen-bonded mutants with $\Delta G_1 = 1000-1500 \text{ cm}^{-1}$ the contribution of the superexchange route is significant¹¹⁷ (i.e., for $\Delta G_1 = 1200 \text{ cm}^{-1}$, $F_{\text{SUP}} = 0.25$ at $T = 300 \text{ K}$ and $F_{\text{SUP}} = 1.0$ at 20 K). Chemical engineering of the RC with the substitution of the accessory bacteriochlorophyll (B) on the A and/or B branch by 13^2-OH-Ni-B (Ni-B) ($\Delta G_1 =$

-1000 cm^{-1})¹¹⁸ or by 3^2-OH-B (B-vinyl) ($\Delta G_1 = 500 \text{ cm}^{-1}$)¹¹⁹ demonstrates the prevalence of the PSSM for B_A -vinyl $\Delta G_1 \cong 500 \text{ cm}^{-1}$ at room temperature, and with $F_{\text{SUPER}} = 0.25$ at $T = 300 \text{ K}$ (Fig. 22), while $F_{\text{SUPER}} = 1.0$ at $T = 80 \text{ K}$.⁸³ The temperature dependence of the lifetime τ_{ET} for primary ET in the chemically substituted B_6 -vinyl RC on the A branch, with the 'transition' from $\tau_{\text{ET}} = 230 \text{ ps}$ in the range $T = 75\text{-}130\text{K}$, to $\tau_{\text{ET}} = 35 \text{ ps}$ at $T = 295 \text{ K}$,¹¹⁹ provides the proof for the prevalence of the parallel mechanism. The PSSM results in an optimization and stability principle for the primary ET in photosynthesis. It allows for efficient ET over a broad range of ΔG_1 , enabling the prevalence of ET in mutants and chemically engineered RC with an extreme range (i.e., $-1500 \text{ cm}^{-1} \leq \Delta G_1 \leq 1500 \text{ cm}^{-1}$) of energy gaps (i.e., over an energy range of $\sim 9 \text{ kcal}$). The PSSM implies a necessary kinetic redundancy, acting as a safety valve for energy changes and insuring the stability of the primary photosynthetic process for different native, mutagenetically and chemically modified RCs.

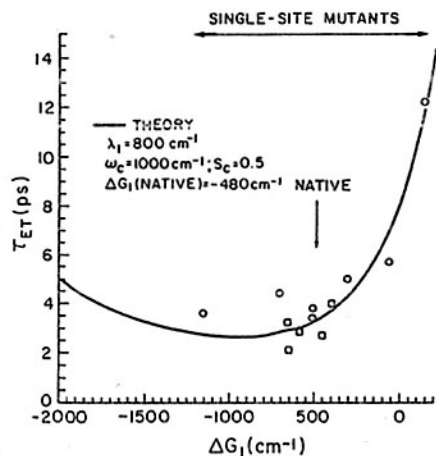
Fig. 20. Model calculations of microscopic ET times from the electronic origin of the doorway DBA manifold coupled in series to the two D^+B^-A and D^+B^-A Franck-Condon quasicontinua, with level structure analogous to Fig. 19 (i.e., $D \equiv P$, $B \equiv B$ and $A \equiv H$). The energy ΔG_1 gap between the DBA and D^+B^-A manifolds is varied in the range -450 cm^{-1} to 450 cm^{-1} . The vibrational frequencies, electronic (V_{DB} and V_{BA}) and nuclear ($\lambda_{DB}, \lambda_{BA}$) couplings are specified on the figure. Note the 'transition' from the sequential to the superexchange domain with increasing ΔG_1 (reference 83).



We proceed from kinetic redundancy to structural redundancy, manifested in the symmetry breaking, i.e., the unidirectionality of the primary charge separation across the A branch. Application of ET theory implies that this unique phenomenon can originate from several contributions, i.e., the electronic couplings and nuclear Franck-Condon factors (determined by energy gap ΔG_1 , medium reorganization

energy, etc.). Modification of the electronic coupling across the B branch leaving ΔG_1 invariant results in too small a contribution for the ratio of the sequential ET rates across the A and B branches, i.e., $k_A/k_B \cong 2-3$.¹¹⁴ The symmetry breaking in the native RC can be induced by the energetic modification of the energy gap $\Delta G_1^{(J)}$ ($J = A, B$) of the P^+B^-H ion pair across the B branch (e.g., $\Delta G_1^{(B)} \geq 1000 \text{ cm}^{-1}$, while $\Delta G_1^{(A)} \cong -500 \text{ cm}^{-1}$). Energetic control then implies that the ET in the (native) RC across the A branch is sequential with $k_A \propto |V_{PB}|^2$, while across branch B it is of superexchange type, i.e., $k_B \propto |V_{PB}V_{BH}/(\Delta G_1^{(B)} + \lambda)|^2$, where V_{PB} and V_{BH} are the appropriate electronic coupling matrix elements. The branching ratio is $k_A/k_B \cong (\Delta G_1^{(B)} + \lambda)^2 / V_{BH}^2 \sim 10^3$. Unidirectionality is then dominated by a cumulative contribution with energy control (i.e., the difference $|\Delta G_1^{(A)} - \Delta G_1^{(B)}|$), modifying the nature of the electronic coupling. Breaking of the symmetry breaking, i.e., inducing charge separation across the B branch can be realized by a chemical modification of the energy gap $\Delta G_1^{(A)}$, retarding the ET process across the A branch.¹²⁰

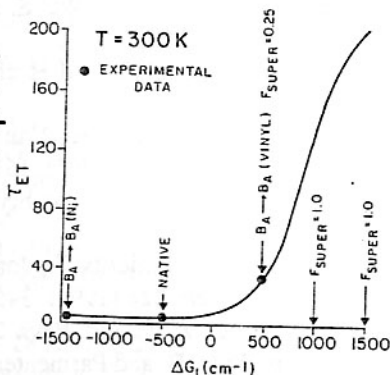
Fig. 21. Theoretical dependence of the free energy relationship or the ET lifetime ($\tau_{ET} = k_{ET}^{-1}$ at $T = 295 \text{ K}$) of the decay of $^1P^+$ in the native RC and some of its single site mutants (which modify ΔG_1 for the $^1P^+/P^+$ energetics). The solid curve presents the nonadiabatic multiphonon theory for sequential ET (in the range $\Delta G_1 = -1500 - 0 \text{ cm}^{-1}$), which involves protein and intramolecular nuclear modes (ref. 117).



The structure of the photosynthetic bacterial RC constituted a seminal accomplishment. Nevertheless, we should challenge the notion of the structure-function relationship, providing a complete description of the central energy conversion process in photobiology. Structural information alone is not sufficient to understand the function of the RC, which rests on the ingredients of ultrafast

dynamics. Dynamic information transcends and complements structural data. We should strive towards the broad unification of structure-dynamics-function relations in ultrafast biophysical and chemical dynamics.

Fig. 22. Application of the parallel sequential-superechange model to chemically engineered RCs at 300K. The ΔG_1 dependence of the experimental ET lifetime (\bullet) $\tau_{ET} = k_{ET}^{-1}$ of the decay of $^1P^*$ in the native RC and in the chemically modified Ni-B (ref. 118) and B-vinyl ref. 119) RCs, are accounted for (solid curve) by the PSSM model. F_{SUPER} represent the calculated superechange branching ratio.



Acknowledgment

The Swedish science community made seminal contributions to international science communication since J. Berzelius served as the permanent Secretary of the Royal Swedish Academy of Sciences, publishing the Annual Reports on the Progress of Science.¹²¹ It was a privilege to contribute to the Nobel Symposium on Femtochemistry and Femtobiology, which constituted an important scientific endeavour.

References

1. Bonhoeffer K. F. and Farkas L., *Z. Phys. Chem.* 134 (1928), 337.
2. Wenzel G., *Z. Phys.* 29 (1928), 321.
3. Eyring H. and Polanyi M., *Z. Phys. Chem.* B12 (1931), 279.
4. Levine R. D. and Bernstein R. B., *Molecular Reaction Dynamics* (Oxford University Press, New York, 1987).
5. Kubo R. and Toyozawa Y., *Prog. Theoret. Phys.* 13 (1955), 160.
6. Marcus, R. A., *J. Chem. Phys.* 24 (1956), 966, 979.
7. Förster Th., *Discuss. Farad. Soc.* 27 (1959), 7.
8. DeVault D. and Chance B., *Biophys. J.* 6 (1966), 825.
9. Smalley R. E., Wharton L. and Levy D. H., *J. Chem. Phys.* 64 (1976), 3266.
10. Johnson K. E., Wharton L. and Levy D. H., *J. Chem. Phys.* 69 (1978), 2719.
11. Zewail A. H., *Femtochemistry* (World Scientific, Singapore, 1994).

12. *Femtosecond Chemistry*, eds. Manz J. and Wöste L. (VCH Publishers, Weinheim, 1995).
13. Bersohn R. and Zewail A. H., *Ber. Bunsenges. Phys. Chem.* **92** (1988), 373.
14. Bernstein R. B. and Zewail A. H., *J. Chem. Phys.* **90** (1989), 829.
15. Jortner J. and Levine R. D., *Isr. J. Chem.* **30** (1990), 207.
16. Purnell J., Snyder E. M., Wei S. and Castelman A. W., *Chem. Phys. Lett.* **229** (1994), 333.
17. Wynné K., Reid G. D. and Hochstrasser R. M., *J. Chem. Phys.* **105** (1996), 2287.
18. Bradforth S. E., Jimenez R., Van Mourik F., Van Grondelle R. and Fleming G. R., *J. Phys. Chem.* **99** (1995), 16179.
19. Vos M. H., Rappaport F., Lambry J. C., Breton J. and Martin J. L., *Nature* **363** (1993), 320.
20. Chachisvilis M., Pullerits T., Jones M. R., Hunger C. N. and Sundström V., *Chem. Phys. Lett.* **224** (1994), 345.
21. Coulson C. A., *Rev. Mod. Phys.* **32** (1960), 170.
22. Kistiakowski G. B. and Parmenter C. S., *J. Chem. Phys.* **42** (1965), 2942.
23. Pauling L. and Wilson E. B., *Introduction to Quantum Mechanics* (McGraw Hill, New York, 1935), 322.
24. Jablonski A., *Nature* **131** (1933), 839.
25. Jortner J. and Berry R. S., *J. Chem. Phys.* **48** (1968), 2757.
26. Bixon M., Dothan Y. and Jortner J., *Mol. Phys.* **17** (1969), 109.
27. Van der Meer B. J., Jonkman H. T., Ter Horst G. M., and Kommandeur J., *J. Chem. Phys.* **76** (1982), 2099.
28. Felker P. M., Lambert W. R., and Zewail A. H., *Chem. Phys. Lett.* **89** (1982), 309.
29. Bixon M. and Jortner J., *J. Chem. Phys.* **48** (1968), 715.
30. Bixon M. and Jortner J., *Mol. Cryst.* **213** (1969), 237.
31. Bixon M. and Jortner J., *Isr. J. Chem.* **7** (1969), 189.
32. Bixon M. and Jortner J., *J. Chem. Phys.* **50** (1969), 3284.
33. Bixon M. and Jortner J., *J. Chem. Phys.* **50** (1969), 4061.
34. Jortner J., Rice S. A., and Hochstrasser R. M., *Adv. in Photochem.*, eds. Pitts B. O. and Hammond G. (John Wiley, New York, 1969).
35. Herzberg G., *J. Chim. Phys.* Special Issue "Transitions Non-Radiatives dans les Molecules" (1970), 244.
36. Jortner J., *J. Chim. Phys.* Special Issue "Transitions Non-Radiatives dans les Molecules" (1970), 9.
37. Teller E., *Isr. J. Chem.* **7** (1969), 227.
38. Englman R. and Jortner J., *Mol. Phys.* **18** (1970), 145.
39. Freed K. F. and Jortner J., *J. Chem. Phys.* **52** (1970), 6272.
40. Jortner J., *Pure Appl. Chem.* **24** (1970), 1675.

41. Bixon M., Jortner J., Cortes J., Heitele H. and Michel-Beyerle M. E., *J. Phys. Chem.* **98** (1994), 7289.
42. Jortner J. and Mukamel S., *MTP International Review of Science*, eds. Buckingham A. D. and Coulson C. A. (Butterworth, London, 1976), Vol. 13, p. 327.
43. Nitzan A. and Jortner J., *J. Chem. Phys.* **55** (1971), 1355.
44. Nitzan A., Jortner J. and Rentzepis P. M., *Mol. Phys.* **22** (1971), 585.
45. Nitzan A., Jortner J. and Rentzepis P. M., *Proc. R. Soc. (London)* **A327** (1972), 367.
46. Nitzan A. and Jortner J., *Mol. Phys.* **24** (1972), 109.
47. Nitzan A. and Jortner J., *J. Chem. Phys.* **57** (1972), 2870.
48. Berne B., Nitzan A. and Jortner J., *J. Chem. Phys.* **61** (1974), 227.
49. Jortner J. and Mukamel S., *The World of Quantum Chemistry*, eds. Daudel R. and Pullman B. (Reidel publ. Co., Dordrecht, 1974), 145.
50. Jortner J. and Mukamel S., *Excited States*, ed. Lim E. C. (Academic Press, New York, 1977), vol. III, p. 57.
51. Kommandeur J. and Jortner J., *Chem. Phys.* **28** (1978), 273.
52. Jortner J. and Levine R. D., *Advances in Chemical Physics* (Wiley, New York, 1981), vol. 47, pp 1-114.
53. Amirav A. and Jortner J., *J. Chem. Phys.* **81** (1984), 4200.
54. Even U. and Jortner J., *J. Chem. Phys.* **77** (1982), 4391.
55. Even U., Magen J., Friedman J. and Jortner, J., *J. Chem. Phys.* **77** (1982), 4384.
56. Amirav A., Sonnenschein M. and Jortner, J., *J. Chem. Phys.* **82** (1982), 4378.
57. Amirav A. and Jortner J., *J. Chem. Phys.* **82** (1985), 4378.
58. Jortner J. and Leach S., *J. Chim. Phys.* **77** (1980), 1, 43.
59. Hinshelwood C. N., *Proc. Roy. Soc. (London)* **A113** (1927), 230.
60. Hinshelwood C. N. and Fletcher C. J. M., *Nature* **131** (1933), 24.
61. Jortner J. and Levine R. D. *Mode Selective Chemistry*, eds. Jortner J., Levine R. D. and Pullman B. (Kluwer Academic Publishers, Dordrecht, 1991), 535.
62. Amirav A. and Jortner J., *Chem. Phys. Lett.* **132** (1986), 335.
63. Amirav A., Horowitz C. and Jortner J., *J. Chem. Phys.* **88** (1988), 3092.
64. Marcus R. and Sutin N., *Biochem. Biophys. Acta* **811** (1985), 275.
65. Jortner J., Bixon m., Heitele H. and Michel-Beyerle, M. E., *Chem. Phys. Lett.* **197** (1992), 131.
66. Jortner J., Bixon M., Wegewijs B., Verhoeven J. W. and Rettschnick R. P. H., *Chem. Phys. Lett.* **205** (1993), 451.
67. Bixon M. and Jortner J., *J. Phys. Chem.* **97** (1993), 13061.
68. Jortner J. and Bixon M., *J. Photochem. Photobiol.* **A82** (1994), 5.
69. Meyers A. B., *Chem. Rev.* **96** (1996), 911.
70. Cortes J., Heitele H. and Jortner J., *J. Phys. Chem.* **98** (1994), 2527.

71. Wegewijs B. and Verhoeven J. W., *Adv. Chem. Phys.* (1997), in press.
72. Wegewijs B., Hermant R. M., Verhoeven J. W., Kunst A. G. M. and Rettschnick R. P. H., *Chem. Phys. Lett.* **140** (1987), 587.
73. Wegewijs B., Ng A. K. F., Rettschnick, R. P. H. and Verhoeven J. W., *Chem. Phys. Lett.* **200** (1992), 357.
74. Chaiken O. J., Gurnick M. and McDonald J. D., *J. Chem. Phys.* **74** (1981), 106, 117.
75. Felkér P. M. and Zewail A. H., *J. Chem. Phys.* **82** (1985), 2961, 2975.
76. Saigusa H. and Lim E. C., *J. Chem. Phys.* **78** (1983), 91; **79** (1983), 5223.
77. Hack E. and Huber J. R., *Int. Rev. Phys. Chem.* **10** (1991), 287.
78. Bixon M. and Jortner J., *J. Chem. Phys.* **102** (1994), 5636.
79. Bixon M. and Jortner J., *Mol. Phys.* **89** (1996), 373.
80. Bixon M. and Jortner J., *J. Phys. Chem.* **100** (1996), 11914.
81. Herzberg G., *Spectra of Diatomic Molecules* (Van Nostrand, Princeton, 1945).
82. Bixon M. and Jortner J., *J. Chem. Phys.* (in press).
83. Bixon M. and Jortner J. (to be published).
84. Mies F. H. and Kraus M., *J. Chem. Phys.* **45** (1966), 4455.
85. McLaughlin I., Rice S. A. and Jortner J., *J. Chem. Phys.* **49** (1968), 2756.
86. Schek I. and Jortner J., *J. Chem. Phys.* **70** (1979), 3016.
87. Carmeli B. and Nitzan A., *J. Chem. Phys.* **72** (1980), 2054.
88. Carmeli B., Schek I., Nitzan A. and Jortner J., *J. Chem. Phys.* **72** (1980), 1928.
89. Zewail A. H. (this volume).
90. Last I., Schek I. and Jortner J. (to be published).
91. Hoare M. R., *Adv. Chem. Phys.* **40** (1969), 49.
92. Novick S. E., David P. B. and Klemperer W., *J. Chem. Phys.* **59** (1973), 2273.
93. Beswick J. A. and Jortner J., *Chem. Phys. Lett.* **49** (1977), 13.
94. Beswick J. A. and Jortner J., *J. Chem. Phys.* **68** (1978), 2277.
95. Beswick A. and Jortner J., *Advances in Chemical Physics* (Wiley, New York, 1981), Vol. 47, p. 363.
96. Gutman M., Willberg D. M. and Zewail A. H., *J. Chem. Phys.* **97** (1992), 8038.
97. Jortner J., *Z. Phys. D.* **24** (1992), 247.
98. Jortner J., Even U., Goldberg A., Schek I., Raz T. and Levine R. D., *Surf. Rev. and Lett.* **3** (1996), 263.
99. Jortner J., *J. Chim. Phys.* **92** (1995), 205.
100. Scharf D., Jortner J. and Landman U., *J. Chem. Phys.* **88** (1988), 4273.
101. Buck U. and Krohne R., *Phys. Rev. Lett.* **73** (1994), 947.

102. Schek I., Raz. T., Levine R. D. and Jortner J., *J. Chem. Phys.* 101 (1995), 8390.
103. Rosenblit M. and Jortner J., *Phys. Rev. Lett.* 75 (1995), 4079; *J. Phys. Chem.* (in press).
104. Libby W. F., Abstract 117, *Division of Physical and Inorganic Chemistry, 115th Meeting of the American Chemical Society* (San Francisco, 1949).
105. Kestner N. R., Logan J. and Jortner J., *J. Phys. Chem.* 78 (1974), 2148.
106. Ulstrup J. and Jortner J., *J. Chem. Phys.* 63 (1975), 4358.
107. Bixon M. and Jortner J., *Chem. Phys.* 176 (1993), 467.
108. Kaufman K. J., Dutton P. L., Netzel T. L., Leigh J. S. and Rentzepis, P. M., *Science* 188 (1975), 1301.
109. Rockley M. G., Winsdor M. W., Cogdell R. J. and Parson W. A., *Proc. Natl. Acad. Sci. USA* 72 (1975), 2251.
110. Jortner J., *J. Chem. Phys.* 64 (1976), 4860.
111. Jortner J., *J. Am. Chem. Soc.* 102 (1980), 6676.
112. Jortner J., *Biochim. Biophys. Acta* 594 (1980), 193.
113. Deisenhofer J., Epp O., Miki K., Huber R. and Michel H., *Nature* 318 (1985), 618.
114. Michel-Beyerle M. E., Plato M., Deisenhofer J., Michel H., Bixon M. and Jortner J., *Biochim. Biophys. Acta* 932 (1988), 52.
115. Marcus R. A., *Isr. J. Chem.* 28 (1988), 205.
116. Bixon M., Jortner J. and Michel-Beyerle M. E., *Biochem. Biophys. Acta* 1056 (1991), 301.
117. Bixon M., Jortner J. and Michel-Beyerle M. E., *Chem. Phys.* 197 (1995), 389.
118. Hartwick G., Friese M., Scheer H., Ogrodnick A. and Michel-Beyerle M. E., *Chem. Phys.* 197 (1995), 423.
119. Müller P., Bieser G., Hartwick G., Langenbacher T., Lossau H., Ogrodnik A. and Michel-Beyerle M. E. (in press).
120. Michel-Beyerle M. E. (private communication and to be published).
121. Berzelius J., *Rapport Annuel sur les Progres des Sciences Physiques et Chimiques* (Portin Mason et Co., Paris, 1841).